

# Prediction of Strong Ground Motion Using the Hybrid Empirical Method and Its Use in the Development of Ground-Motion (Attenuation) Relations in Eastern North America

by Kenneth W. Campbell

**Abstract** Ground-motion (attenuation) relations are used to estimate strong ground motion for many engineering and seismological applications. Where strong-motion recordings are abundant, these relations are developed empirically from strong-motion recordings. Where recordings are limited, they are often developed from seismological models using stochastic and theoretical methods. However, there is a large degree of uncertainty in calculating absolute values of ground motion from seismological models in regions where data are sparse. As an alternative, I propose a hybrid empirical method that uses the ratio of stochastic or theoretical ground-motion estimates to adjust empirical ground-motion relations developed for one region to use in another region. By using empirical models as its basis, the method taps into the vast amount of observational data and expertise that has been used to develop empirical ground-motion relations in high-seismic regions such as western North America (WNA). I present a formal mathematical framework for the hybrid empirical method and apply it to the development of ground-motion relations for peak ground acceleration and acceleration response spectra in eastern North America (ENA) using empirical relations from WNA. The application accounts for differences in stress drop, source properties, crustal attenuation, regional crustal structure, and generic-rock site profiles between the two regions. The resulting hybrid empirical ground-motion relations are considered to be most appropriate for estimating ground motion on ENA hard rock with a shear-wave velocity of 2800 m/sec for earthquakes of  $M_w \geq 5.0$  and  $r_{rup} \leq 70$  km. However, it has been extended to larger distances using stochastic ground-motion estimates so that it can be used in more general engineering applications such as probabilistic seismic hazard analysis.

## Introduction

A ground-motion relation, or what is referred to as an attenuation relation by many engineers and seismologists, is often used to estimate strong ground motion for site-specific and regional seismic hazard analyses. It is a simple mathematical model that relates a given ground-motion parameter to several seismological parameters of an earthquake such as magnitude, source-to-site distance, style of faulting, and local site conditions (Campbell, 2002, 2003). The ground-motion parameters that are most commonly predicted by these relations are peak ground acceleration (PGA), peak ground velocity (PGV), and pseudoabsolute response spectral acceleration (PSA). In areas such as western North America (WNA) and Japan where strong-motion recordings are abundant, ground-motion relations are usually developed from empirical methods. However, in many regions of the world, including eastern North America (ENA), there are too few strong-motion recordings with which to develop reliable

empirical ground-motion relations. In these latter regions it has been common practice to predict quantitative ground-motion parameters from qualitative measures of ground shaking such as modified Mercalli intensity (MMI) or Medvedev–Spooner–Karnik intensity using what I refer to as the intensity method. The intensity method is applied by first predicting seismic intensity from an intensity ground-motion relation, then estimating the ground-motion parameter of interest from a relationship between ground motion and seismic intensity (e.g., Trifunac and Lee, 1989, 1992; Wald *et al.*, 1999; Atkinson and Sonley, 2000; Atkinson, 2001a).

When the number of strong-motion recordings is limited but good seismological network data are available, it is possible to derive simple seismological models that can be used to describe how ground motion scales with earthquake source size and source-to-site distance. This concept led McGuire and Hanks (1980) and Hanks and McGuire (1981)

to propose a point-source stochastic method, later generalized and extended by Boore (1983), that could be used to estimate ground motion from such simple seismological models. Because of its success and simplicity, the point-source stochastic method is now widely used to predict strong ground motion in many regions of the world where the number of strong-motion recordings is limited (see Boore [2003] for a comprehensive list of these applications and a summary of the stochastic method). With the improvement of computers, it has become possible to use more sophisticated numerical methods for simulating strong ground motion based on empirical and theoretical source functions and two- and three-dimensional wave propagation theory (e.g., see summaries in Somerville [1993] and Anderson [2003]), which I refer to as the theoretical method. However, I am aware of only one generalized ground-motion relation (i.e., one that includes both magnitude and distance as seismological parameters) that has been developed using this method (Somerville *et al.*, 2001).

Many ground-motion relations developed using the point-source stochastic method lack the near-source ground-motion characteristics inherent in empirical ground-motion relations, most notably magnitude saturation. Also, because of their reliance on a common method, ground-motion relations developed by different investigators using the point-source stochastic method could possibly lead to an underestimation of epistemic uncertainty (uncertainty in scientific knowledge) if this uncertainty is based solely on differences in the median ground-motion estimates from these relations. Providing a robust assessment of epistemic uncertainty is an important element in the engineering estimation of design ground motion (Budnitz *et al.*, 1997; Savy *et al.*, 1999; Stepp *et al.*, 2001). The sole reliance on the point-source stochastic method of the commonly used ENA ground-motion relations (e.g., Atkinson and Boore, 1995, 1997; Frankel *et al.*, 1996; Toro *et al.*, 1997) led me to propose an alternative hybrid empirical method based on principles that have evolved over the last three decades. The hybrid empirical method uses adjustment factors based on seismological models to estimate ground motions in a region where the number of strong-motion recordings is limited, which I refer to as the target region, from ground-motion estimates in another region where empirical ground-motion relations are available, which I refer to as the host region. In the ENA example presented later, the adjustment factors are developed from the ratio of stochastic ground-motion estimates, so they should be less dependent on the specific parameters of the stochastic models in each region. This is due to their being based on the differences in the source, path, and site parameters between the host and target regions and not on the absolute values of these parameters.

In this article I develop the mathematical basis for the hybrid empirical method, then apply it to developing PGA and PSA ground-motion relations for ENA using empirical ground-motion relations from WNA. These new hybrid empirical ground-motion relations are shown to be similar to

other ENA relations that were developed using the point-source stochastic method outside of the near-source regime. However, because of their reliance on well-constrained empirical models, they provide more realistic near-source attenuation characteristics that cannot be obtained from the point-source stochastic method alone without including finite-fault effects (Beresnev and Atkinson, 1999, 2002; Atkinson and Silva, 2000; Gregor *et al.*, 2002) or imposing constraints on geometrical attenuation, stress drop, or hypocentral depth (Frankel *et al.*, 1996, 2002; Silva *et al.*, 2002). This assumes that near-source characteristics similar to those observed in the host region are expected to occur in the target region.

## Background

Campbell (1981) introduced a simple semiempirical procedure for developing a PGA ground-motion relation in ENA that was an alternative to the intensity method that served as the standard at the time (see Campbell [1986] for a review of the intensity method). He used adjustment factors based on simple seismological models to account for differences in anelastic attenuation and regional magnitude measures between WNA and ENA. This was the first application of what would later be called the hybrid empirical method. A year later Campbell (1982) used the same method to develop a PGA ground-motion relation for Utah. Campbell (1987, 2000a) applied a more sophisticated version of the hybrid empirical method to develop PGA and PGV ground-motion relations for north-central Utah from those in WNA taking into account differences in stress regime, style of faulting, anelastic attenuation, and local site conditions. He used these relations to estimate a near-source response spectrum and its epistemic uncertainty for a large postulated earthquake on the Wasatch fault in the vicinity of Salt Lake City using the design spectral shapes recommended by Newmark and Hall (1982).

The refinement of the hybrid empirical method began in the early 1990s, when I was asked by the U.S. Nuclear Regulatory Commission (NRC) to develop alternative spectral ground-motion relations for use in the probabilistic risk assessments of two nuclear facilities in WNA. The NRC staff wanted to use these hybrid empirical relations to supplement the point-source stochastic models that the facility operators were using at the time. Partly based on its success in these studies, it was later selected as one of several methods used by experts to evaluate PGA, PGV, and spectral acceleration for the probabilistic seismic hazard analyses being conducted as part of the Senior Seismic Hazard Analysis Committee (SSHAC) Project (Budnitz *et al.*, 1997), Trial Implementation Project (Savy *et al.*, 1999), and Yucca Mountain High-Level Radioactive Waste Repository Project (Stepp *et al.*, 2001). For these applications the hybrid empirical method took into account regional differences in stress drop, magnitude measures, style of faulting, anelastic attenuation,

crustal velocity structure, and local site conditions between WNA and either southeastern ENA or southwestern Nevada.

The first formal mathematical framework of the model was published as part of the documentation of the Yucca Mountain Project (Stepp *et al.*, 2001) and later in a 1999 Nuclear Energy Agency workshop (Campbell, 2001a) and U.S. Geological Survey (USGS) research report (Campbell, 2001b) that included example applications to the development of ground-motion relations in ENA. Atkinson and Boore (1998) independently evaluated the hybrid empirical method and concluded that ground-motion relations in California could be reliably modified to predict strong ground motion in ENA from future large earthquakes. Atkinson (2001b) and Abrahamson and Silva (2001) later applied the method to estimate ground motion in ENA.

### Mathematical Framework

Application of the hybrid empirical method requires five steps: (1) selection of the host and target regions, (2) calculation of empirical ground-motion estimates for the host region, (3) calculation of seismological-based adjustment factors between the host and target regions, (4) calculation of hybrid empirical ground-motion estimates for the target region, and (5) development of ground-motion relations.

The host region must have one or more empirical ground-motion relations that can be used to estimate the ground-motion parameters of interest. The use of multiple relations allow for the assessment of epistemic uncertainty. Both regions must also have one or more seismological models that can be used to model their regional source spectra, crustal velocity structure, wave propagation characteristics, and local site characteristics. Empirical ground motions should be calculated for the set of ground-motion parameters, magnitudes, distances, and other seismological parameters that will be included in the hybrid empirical estimates for the target region. The modeled ground motions used to calculate the adjustment factors can be computed using any appropriate ground-motion simulation method. However, the stochastic method should be adequate for most applications.

One of the attributes of the hybrid empirical method is its ability to easily provide estimates of aleatory variability and epistemic uncertainty in the predicted ground motion. Aleatory variability results from the inherent randomness in the predicted ground-motion parameter. This randomness can be caused by unknown or unmodeled characteristics of the underlying physical process that causes the ground motion. Epistemic uncertainty results from a lack of scientific knowledge in the equations, algorithms, and parameters that are used to model this physical process. In the mathematical formulation given below, I use a lognormal probability distribution to describe the aleatory variability and epistemic uncertainty in the ground-motion predictions and a Gaussian distribution to describe the epistemic uncertainty in the aleatory variability. Following the convention of Benjamin and

Cornell (1970), I refer to the mean of the natural logarithm of a ground-motion parameter as its median. All of the standard deviations of ground motion are given in terms of the natural logarithm.

The median hybrid empirical ground-motion estimate for the target region is given by

$$\ln \check{y}^t(\beta_{jk}) = \sum_{i=1}^n [w_i(\beta_{jk}) \ln y_i^t(\beta_{jk})], \quad (1)$$

where

$$\ln y_i^t(\beta_{jk}) = \ln y_i^h(\beta_{jk}) + \ln \check{F}(\beta_{jk}). \quad (2)$$

The superscripts “t” and “h” refer to the target and host regions, respectively;  $n$  is the total number of empirical ground-motion relations;  $\beta_{jk}$  is the  $k$ th value of the  $j$ th seismological parameter, where  $k$  quantifies epistemic uncertainty;  $\ln y_i^h(\beta_{jk})$  is the  $i$ th empirical ground-motion estimate in the host region;  $\check{F}(\beta_{jk})$  is the median value of the modeled adjustment factor between the host and target regions; and  $w_i(\beta_{jk})$  is a set of weights whose sum over  $i$  must equal unity. Multiple empirical ground-motion relations are used to estimate  $\ln y_i^h(\beta_{jk})$  in order to quantify epistemic uncertainty. The weights are allowed to vary by ground-motion relation, seismological parameter, and parameter values. The set of seismological parameters used in the predictions should take into account the distribution of magnitude, distance, style of faulting, local site characteristics, and other seismological parameters that will eventually be used in the development of the ground-motion relations in the target region.

The median value of the adjustment factor is given by

$$\begin{aligned} \ln \check{F}(\beta_{jk}) &= \sum_{l=1}^{n1} \sum_{m=1}^{n2} \sum_{o=1}^{n3} \sum_{p=1}^{n4} [w(\phi_{lm}^t) w(\phi_{op}^h) \ln F(\beta_{jk}, \phi_{lm}^t, \phi_{op}^h)], \end{aligned} \quad (3)$$

where

$$\ln F(\beta_{jk}, \phi_{lm}^t, \phi_{op}^h) = \ln Y^t(\beta_{jk}, \phi_{lm}^t) - \ln Y^h(\beta_{jk}, \phi_{op}^h). \quad (4)$$

$Y^t(\beta_{jk}, \phi_{lm}^t)$  is the modeled ground-motion estimate in the target region;  $Y^h(\beta_{jk}, \phi_{op}^h)$  is the modeled ground-motion estimate in the host region;  $\phi_{lm}^t$  is the  $m$ th value of the  $l$ th model parameter in the target region, where  $m$  quantifies epistemic uncertainty;  $w(\phi_{lm}^t)$  is the weight corresponding to  $\phi_{lm}^t$ , which must equal unity when summed over  $m$ ;  $\phi_{op}^h$  is the  $p$ th value of the  $o$ th model parameter in the host region, where  $o$  quantifies epistemic uncertainty;  $w(\phi_{op}^h)$  is the weight corresponding to  $\phi_{op}^h$ , which must equal unity when summed over  $p$ ; and  $n1$ ,  $n2$ ,  $n3$ , and  $n4$  are the numbers of model parameters or their alternative values.  $\phi_{lm}^t$  and  $\phi_{op}^h$  include those seismological parameters that are required to estimate  $Y^t(\beta_{jk}, \phi_{lm}^t)$  and  $Y^h(\beta_{jk}, \phi_{op}^h)$  but are not explicitly included in the parameter set  $\beta_{jk}$ . Stress drop and crustal at-

tenuation are typical examples of such parameters. In this general formulation the model parameters in the host region,  $\phi_{op}^h$ , are assumed to have epistemic uncertainty. However, in many applications this uncertainty is expected to be relatively small compared to the epistemic uncertainty in  $\phi_{lm}^t$  and can be neglected. This is because the values of the model parameters in the host region will usually be well constrained by strong-motion recordings and seismological network data. If this is not the case, then this uncertainty should not be neglected. The summations in equation (3) assume that the values of the model parameters in the host and target regions are uncorrelated.

Equation (3) is structured as if  $\phi_{lm}^t$  and  $\phi_{op}^h$  are defined by a discrete set of values or models (defined by the indices  $m$  and  $p$  in the above equations) with weights  $w(\phi_{lm}^t)$  and  $w(\phi_{op}^h)$ . Discrete distributions are typically used in the development of a logic tree (e.g., Thenhaus and Campbell, 2002). It is also possible to model continuous variables in this way as long as they can be defined by a relatively small number of discrete values and corresponding weights. If the number of alternative parameter values or logic-tree branches becomes very large, it is more efficient to sample  $\phi_{lm}^t$  and  $\phi_{op}^h$  using a Monte Carlo simulation, in which case they can be defined by either discrete or continuous probability distributions (e.g., Thenhaus and Campbell, 2002).

The mean aleatory standard deviation of  $\ln \check{y}^t(\beta_{jk})$  is given by

$$\bar{\sigma}_{\ln y}^t(\beta_{jk}) = \sum_{i=1}^n [w_i(\beta_{jk}) \sigma_i^t(\beta_{jk})], \quad (5)$$

where

$$\sigma_i^t(\beta_{jk}) = [(\sigma_i^h(\beta_{jk}))^2 + (\delta\sigma_i^h)^2]^{1/2}; \quad (6)$$

$\sigma_i^h(\beta_{jk})$  is the aleatory standard deviation of  $\ln y_i^h(\beta_{jk})$ ,  $\delta\sigma_i^h$  is the additional aleatory standard deviation that comes from excluding one or more seismological parameters when evaluating the empirical ground-motion relations, and all other variables are defined in equation (1). Seismological parameters that might contribute to  $\delta\sigma_i^h$  are those that model style-of-faulting and hanging-wall effects since these effects might not be appropriate for evaluating ground motions in the target region.

The epistemic standard deviation of  $\ln \check{y}^t(\beta_{jk})$  is given by

$$\tau_{\ln y}^t(\beta_{jk}) = \left\{ (\tau_F(\beta_{jk}))^2 + \sum_{i=1}^n [w_i(\beta_{jk}) (\ln y_i^t(\beta_{jk}) - \ln \check{y}^t(\beta_{jk}))^2] \right\}^{1/2}, \quad (7)$$

where  $\tau_F(\beta_{jk})$  is the epistemic standard deviation of  $\ln \check{F}(\beta_{jk})$ . This later standard deviation accounts for uncertainty in the modeled adjustment factors that is not accounted for in the

aleatory standard deviation defined in equation (5). It is given by

$$\tau_F(\beta_{jk}) = \left\{ \sum_{l=1}^{n1} \sum_{m=1}^{n2} \sum_{o=1}^{n3} \sum_{p=1}^{n4} [w(\phi_{lm}^t) w(\phi_{op}^h) (\ln F(\beta_{jk}, \phi_{lm}^t, \phi_{op}^h) - \ln \check{F}(\beta_{jk}))^2] \right\}^{1/2}. \quad (8)$$

If desired the total dispersion in an individual estimate of  $\ln \check{y}^t(\beta_{jk})$  can be calculated by combining the aleatory and epistemic standard deviations by the square root of sum of squares, giving

$$\sigma_{\text{tot}}^t(\beta_{jk}) = [(\bar{\sigma}_{\ln y}^t(\beta_{jk}))^2 + (\tau_{\ln y}^t(\beta_{jk}))^2]^{1/2}. \quad (9)$$

The epistemic standard deviation of  $\bar{\sigma}_{\ln y}^t(\beta_{jk})$  is given by

$$\tau_{\sigma}^t(\beta_{jk}) = \left\{ \sum_{i=1}^n [w_i(\beta_{jk}) (\sigma_i^t(\beta_{jk}) - \bar{\sigma}_{\ln y}^t(\beta_{jk}))^2] \right\}^{1/2}. \quad (10)$$

Although it is rarely used except for analyses involving high-risk facilities (e.g., Savy *et al.*, 1999; Stepp *et al.*, 2001), the relation for  $\tau_{\sigma}^t(\beta_{jk})$  is included here for completeness.

### Ground-Motion Relations for ENA

I used the hybrid empirical method to develop PGA and PSA ground-motion relations for ENA hard rock based on the general approach adopted for the Trial Implementation Project (Savy *et al.*, 1999). For the target region, I selected that part of ENA described by Toro *et al.* (1997) as the Mid-continent region. It generally includes the region of North America bounded on the west by the Rocky Mountains and on the south by the Gulf Coast. ENA is a good candidate for the hybrid empirical method because, although it has few strong-motion recordings (especially at moderate to large magnitudes of greatest interest), it has been well studied by seismologists. I selected WNA as the host region because it has a large number of reliable empirical attenuation relations and it has been well studied by seismologists. For purposes of this application, WNA is generally defined as the shallow crustal region of North America located west of the Sierra Nevada and Cascade Mountains. Most of the strong-motion recordings in this region come from California, although many of the empirical attenuation relations developed for this region include some worldwide recordings from tectonic environments similar to WNA.

I selected four WNA empirical ground-motion relations, designated  $y_i^{\text{wna}}(\beta_{jk})$ , and their corresponding aleatory standard deviations,  $\sigma_i^{\text{wna}}(\beta_{jk})$ . Note that the generic superscript “h” used to identify the host region in the general mathematical formulation is now replaced by “wna” to designate WNA as the host region. Similarly the superscript “t” is replaced by “ena” to designate ENA as the target region. The

four selected empirical ground-motion relations are Abrahamson and Silva (1997), Campbell (1997), Sadigh *et al.* (1997), and Campbell and Bozorgnia (2003). All of these relations are widely used in engineering and engineering seismology and collectively represent a wide range of differing opinions concerning their mathematical forms, databases, and regression techniques. One of the critical constraints of the hybrid empirical method is that the selected empirical relations should have physically realistic geometrical and anelastic attenuation characteristics. Otherwise, application of the modeled adjustment factors can lead to greatly biased attenuation characteristics in the target region, often leading to predicted ground motions that can increase rather than decrease with distance at large distances (e.g., Atkinson, 2001b). Of those empirical relations widely used in engineering, only those of Campbell (1997) and Sadigh *et al.* (1997) exhibit realistic attenuation characteristics at distances of around 70 km and greater. The Campbell and Bozorgnia (2003) relation, although it does not constrain the rate of attenuation at large distances, has realistic attenuation characteristics to distances to at least 60 km and is sufficiently different in functional form and predicted values from that of Campbell (1997) to significantly contribute to epistemic uncertainty. The Campbell (1997) relation is used here, even though Campbell and Bozorgnia (2003) suggested that it should be superseded by their new relation, because of its more realistic attenuation characteristics at moderate to large distances. Another critical constraint of the hybrid empirical method is that the empirical ground-motion relations should demonstrate physically realistic magnitude scaling characteristics, especially when extrapolated to large magnitudes and short distances. This is important because one of the uses of ENA ground-motion relations is to estimate the ground motion from great earthquakes in the New Madrid fault zone. The three previously mentioned relations all meet this constraint. The Abrahamson and Silva (1997) relation has the slowest attenuation rate of those selected. It is used nonetheless because of its realistic magnitude scaling characteristics. As demonstrated later, all of the empirical relations were truncated at 70 km to avoid unrealistic predicted attenuation rates in ENA. The Boore *et al.* (1997) relation was not selected because it was found to exhibit both unrealistic attenuation characteristics beyond about 50–100 km and unrealistic magnitude scaling for magnitudes greater than about 7.7. In fact, the authors specifically recommended that it not be used for larger magnitudes and distances, even in WNA.

The ground-motion parameters were defined as the geometric mean (hereafter referred to as the average) of the two horizontal components of PGA and 5% damped PSA at natural periods ranging from 0.02 to 4.0 sec. PGA was assumed to represent the value of PSA at 0.01-sec period. For those ground-motion relations that do not provide spectral values at the shorter periods of interest, I estimated these values using interpolation factors derived from those relations that do. Estimates for such short periods are necessary to estimate

the expected peak in the ENA hard-rock acceleration response spectra. All of the relations define magnitude as moment magnitude,  $M_w$ . The Campbell (1997) and Campbell and Bozorgnia (2003) relations define distance as the closest distance to the seismogenic part of fault rupture,  $r_{\text{seis}}$ . The other two relations define distance as the closest distance to the rupture plane,  $r_{\text{rup}}$ . Collectively  $M_w$ ,  $r_{\text{seis}}$ ,  $r_{\text{rup}}$ , and their corresponding values make up the seismological parameter set  $\beta_{jk}$ . All of the empirical ground-motion estimates were defined in terms of  $r_{\text{rup}}$  for purposes of developing the hybrid empirical ground-motion estimates. I considered the ground-motion variability from all other seismological parameters in the empirical ground-motion relations to be aleatory since in most applications these parameters will not be known or their affect on ground motion is not necessarily the same in ENA as in WNA.

Since all of the empirical ground-motion relations use  $M_w$  to define magnitude, no adjustment for differences in magnitude measures was necessary. The relationship between the two distance measures is generally dependent on the geometry of the assumed rupture plane (Abrahamson and Shedlock, 1997). However,  $r_{\text{seis}}$  can be related to  $r_{\text{rup}}$  for a wide range in rupture geometry by simply setting it to 3 km when  $r_{\text{rup}} < 3$  km. The only situation for which this is not the case is for a site located on the footwall of a dipping fault that ruptures within 3 km of the ground surface. However, such shallow rupture has generally not been observed, nor is it expected to occur in ENA. Empirical ground-motion estimates were made for  $M_w = 5.0$ – $8.2$  in increments of 0.2 and for  $r_{\text{rup}} = r_{\text{seis}} = 1, 2, 3, 5, 7, 10, 20, 30, 40, 50,$  and 70 km.

All of the ground-motion relations were evaluated for local site conditions defined as generic rock by Boore and Joyner (1997). I assumed that the rock categories defined by Abrahamson and Silva (1997) and Sadigh *et al.* (1997) represented generic rock, so no correction was necessary. I evaluated the Campbell (1997) relation for generic rock by setting  $S_{\text{SR}} = 1$ ,  $S_{\text{HR}} = 0$ , and  $D = 1$  (Campbell, 2000b), where  $S_{\text{SR}}$  is the indicator variable for soft rock,  $S_{\text{HR}}$  is the indicator variable for hard rock, and  $D$  is sediment depth. I evaluated the Campbell and Bozorgnia (2003) relation for generic rock by setting  $S_{\text{SR}} = S_{\text{FR}} = 0.5$  and  $S_{\text{VFS}} = 0$ , where  $S_{\text{SR}}$  is the indicator variable for soft rock,  $S_{\text{FR}}$  is the indicator variable for hard rock, and  $S_{\text{VFS}}$  is the indicator variable for very firm soil. All of the ground-motion relations were evaluated for a random or unknown style of faulting by setting  $F_{\text{RV}} = F_{\text{TH}} = 0.25$  in the Campbell and Bozorgnia (2003) relation and  $F = 0.5$  in the other relations, where  $F_{\text{RV}}$  is the indicator variable for reverse faulting,  $F_{\text{TH}}$  is the indicator variable for thrust faulting, and  $F$  is the indicator variable for reverse and thrust faulting. I used a generic style of faulting because I do not know whether similar differences in ground motion between faulting styles can be expected in ENA as in WNA. The hanging-wall factors in the Abrahamson and Silva (1997) and Campbell and Bozorgnia (2003) ground-motion relations were set to  $HW = 0$  since

there is a low probability that a generic site in ENA will be located over the hanging wall of a dipping fault as defined by these authors.

The aleatory standard deviation of each relation,  $\sigma_i^{\text{wna}}(\beta_{jk})$ , was increased by an additional standard deviation,  $\delta\sigma_i^{\text{wna}}$ , for those ground-motion relations in which some of the seismological parameters were treated as random variables. Adjustments were made for the sediment-depth term in the Campbell (1997) relation and for the style-of-faulting terms in all of the relations. No adjustment was made for the hanging-wall terms in the Abrahamson and Silva (1997) and Campbell and Bozorgnia (2003) relations because these terms affect such a small number of recordings that they do not have a measurable impact on the overall aleatory variability. The values of  $\delta\sigma_i^{\text{wna}}$  are listed in Table 1.

Based on its success in modeling a wide range of ground motions (Boore, 2003), I selected the point-source stochastic method and a single-corner  $\omega$ -square source spectrum to estimate the median modeled ground-motion parameters,  $Y^{\text{wna}}(\beta_{jk}, \phi_{op}^h)$  and  $Y^{\text{ena}}(\beta_{jk}, \phi_{lm}^t)$ . I used the computer program SMSIM developed by Boore (1996) to perform the calculations. Atkinson and Boore (1995, 1997), Frankel *et al.* (1996), and Toro *et al.* (1997) also used the point-source stochastic method to develop modeled ground-motion relations for ENA. However, Atkinson and Boore used a double-corner instead of a single-corner source spectrum in their calculations, which results in significantly lower mid- to long-period spectral accelerations at large magnitudes (Atkinson and Boore, 1998). As I discuss later, the difference between a single-corner and a double-corner source spectrum should not have as large an impact on the hybrid empirical method. I developed modeled ground motions for the same values of  $M_w$  and  $r_{\text{rup}}$  that I used to derive the empirical ground-motion estimates assuming that  $r_{\text{rup}}$  corresponds to the distance measure  $R$  used in the point-source stochastic model described later.

The stochastic method assumes that ground motion can be modeled as Gaussian bandlimited noise and uses random process theory in combination with simple seismological models to describe the source, propagation, and site characteristics. The salient features of this method are briefly summarized for completeness. A more thorough description can be found in Boore (1983, 2003). Using notation proposed by Boore (2003), the total Fourier amplitude spectrum of displacement,  $Y(M_0, R, f)$ , is calculated from the earthquake source,  $E(M_0, f)$ , the propagation path,  $P(R, f)$ , the site response,  $G(f)$ , and the instrument or type of motion,  $I(f)$ , from the relation

$$Y(M_0, R, f) = E(M_0, f) P(R, f) G(f) I(f), \quad (11)$$

where  $M_0$  is seismic moment,  $f$  is frequency, and  $R$  is distance. Moment magnitude is related to  $M_0$  by the relationship (Hanks and Kanamori, 1979)

Table 1  
Additional Aleatory Variability Used in the Hybrid Empirical Model

| Period<br>(sec) | Additional Aleatory Standard Deviation, $\delta\sigma_i^{\text{wna}}$ |                |       |
|-----------------|---|----------------|-------|
|                 | Style of Faulting   | Sediment Depth | Total |
| 0.01            | 0.10  | 0              | 0.100 |
| 0.02            | 0.10  | 0              | 0.100 |
| 0.03            | 0.10  | 0              | 0.100 |
| 0.05            | 0.10  | 0              | 0.100 |
| 0.075           | 0.10  | 0              | 0.100 |
| 0.10            | 0.10  | 0              | 0.100 |
| 0.15            | 0.10  | 0              | 0.100 |
| 0.20            | 0.09  | 0              | 0.090 |
| 0.30            | 0.08  | 0              | 0.080 |
| 0.50            | 0.07  | 0.043          | 0.082 |
| 0.75            | 0.06  | 0.064          | 0.088 |
| 1.0             | 0.05  | 0.099          | 0.111 |
| 1.5             | 0.03  | 0.125          | 0.129 |
| 2.0             | 0.02  | 0.144          | 0.145 |
| 3.0             | 0   | 0.149          | 0.149 |
| 4.0             | 0   | 0.182          | 0.182 |

$$M_w = \frac{2}{3} \log M_0 - 10.7, \quad (12)$$

where  $M_0$  has units of dyne cm.

The source term is given by

$$E(M_0, f) = C M_0 S(M_0, f), \quad (13)$$

where  $S(M_0, f)$  is the source displacement spectrum and the constant  $C$  is given by

$$C = \langle R_{\Theta\Phi} \rangle V F / (4\pi\rho_s\beta_s^3 R_0), \quad (14)$$

where  $\langle R_{\Theta\Phi} \rangle = 0.55$  is the shear-wave radiation pattern averaged over the focal sphere,  $V = 1/\sqrt{2}$  is the partition of the total shear-wave energy into two horizontal components,  $F = 2$  is the effect of the free surface,  $\rho_s$  and  $\beta_s$  are the density and shear-wave velocity in the vicinity of the earthquake source, and  $R_0 = 1$  km is a reference distance. The source displacement spectrum for the assumed single-corner  $\omega$ -square source model is given by (Brune, 1970, 1971)

$$S(M_0, f) = \frac{1}{1 + (f/f_0)^2}, \quad (15)$$

where the corner frequency in hertz is given by

$$f_0 = 4.9 \times 10^6 \beta_s (\Delta\sigma/M_0)^{1/3}, \quad (16)$$

where  $\Delta\sigma$  is stress drop in bar,  $\beta_s$  has units of kilometers per second, and  $M_0$  has units of dyne cm.

For this study the path term was calculated by multiplying a point-source geometrical attenuation term,  $Z(R)$ , by a crustal damping term,

$$P(R, f) = Z(R) \exp\left(\frac{-\pi f R}{Q(f)c_Q}\right), \quad (17)$$

where the quality factor,  $Q(f)$ , models anelastic attenuation and scattering within the crust and  $c_Q = \beta_s$  is the seismic velocity used in the determination of  $Q(f)$ . The geometrical attenuation terms are modeled by the piecewise continuous function given in Table 2.

The site term was conveniently separated into its amplification and diminution components,

$$G(f) = A(f)D(f), \quad (18)$$

where for this study the amplification term was calculated by the quarter-wavelength method (Joyner *et al.*, 1981; Boore and Joyner, 1991) given by

$$A(f) = \sqrt{\frac{\rho_s \beta_s}{\bar{\rho}(f) \bar{\beta}(f)}}, \quad (19)$$

where

$$\bar{\rho}(f) = \frac{1}{z(f)} \int_0^{z(f)} \rho(z) dz, \quad (20)$$

and

$$\bar{\beta}(f) = z(f) \left[ \int_0^{z(f)} (1/\beta(z)) dz \right]^{-1}, \quad (21)$$

$$z(f) = \frac{\bar{\beta}(f)}{4f}. \quad (22)$$

In these equations,  $\bar{\rho}(f)$  and  $\bar{\beta}(f)$  are the average density and shear-wave velocity to a depth of a quarter-wavelength,  $z(f)$ , for wave frequency  $f$ ;  $\rho_s$  and  $\beta_s$  are the corresponding properties along the propagation path; and  $\beta(z)$  is the shear-wave velocity at some arbitrary depth,  $z$ . Because of the interdependence of  $\bar{\beta}(f)$  and  $z(f)$ , these two parameters are calculated by iteration.

For this study the diminution term was calculated using the kappa filter (Anderson and Hough, 1984),

$$D(f) = \exp(-\pi \kappa_0 f), \quad (23)$$

where  $\kappa_0$  is a parameter that represents the attenuation of ground motion in the upper few kilometers of the site profile.

The type of ground motion or instrument response depends on the desired ground-motion parameter. The calculation of PGA requires the estimation of the Fourier amplitude spectrum of ground acceleration. The calculation of

Table 2  
Seismological Parameters Used in the WNA and ENA Stochastic Models

| Parameter                                       | Western North America (WNA)                           | Eastern North America (ENA)   |
|---|---|---|
| Source spectrum                                 | Brune $\omega$ -square, point source                  | Brune $\omega$ -square, point source  |
| Stress drop, $\Delta\sigma$ (bar)               | 100   | 105 (0.05),* 125 (0.25), 150 (0.40),<br>180 (0.25), 215 (0.05)  |
| Geometric attenuation                           | $R^{-1}$ ; $R < 40$ km<br>$R^{-0.5}$ ; $R \geq 40$ km | $R^{-1}$ ; $R < 70$ km<br>$R^0$ ; $70 \text{ km} \leq R < 130$ km<br>$R^{-0.5}$ ; $R \geq 130$ km                                     |
| Source duration, $T_s$ (sec)                    | $1/f_0$   | $1/f_0$   |
| Path duration, $T_p$ (sec)                      | $0.05R$   | 0; $R \leq 10$ km<br>$0.16R$ ; $10 \text{ km} < R \leq 70$ km<br>$-0.03R$ ; $70 \text{ km} < R \leq 130$ km<br>$0.04R$ ; $R > 130$ km |
| Path attenuation, $Q$                           | $180f^{0.45}$   | $400f^{0.4}$ (0.3), $680f^{0.36}$ (0.4),<br>$100f^{0.3}$ (0.3)  |
| Shear velocity, $\beta_s$ (km/sec)              | 3.5   | 3.6   |
| Density, $\rho_s$ (g/cc)                        | 2.8   | 2.8   |
| Site attenuation, $\kappa_0$ (sec)              | 0.04  | 0.003 (0.3), 0.006 (0.4), 0.012 (0.3)   |
| Site amplification method <sup>†</sup>          | Quarter-wavelength                                    | Quarter-wavelength  |
| Local site profile <sup>‡</sup> (30-m velocity) | WNA generic rock<br>(620 m/sec)                       | ENA hard rock (2800 m/sec)  |

\*Where multiple values are used, weights are given in parentheses.

<sup>†</sup>Site amplification terms are given in Table 4.

<sup>‡</sup>Crustal velocity models are given in Table 3.

PSA requires the estimation of the Fourier amplitude spectrum of pseudoacceleration response. The response term for ground acceleration is given by

$$I(f) = (2\pi f)^2, \quad (24)$$

and that for pseudoacceleration is given by

$$I(f) = \frac{(2\pi f f_r)^2}{[(f^2 - f_r^2)^2 - (2f f_r \zeta)^2]^{1/2}}, \quad (25)$$

where  $f_r$  and  $\zeta$  are the undamped natural frequency and critical damping ratio of a single-degree-of-freedom system.

Given the appropriate form for  $I(f)$ , I calculated the expected value of PGA and 5% damped PSA from  $Y(M_0, R, f)$  using random process theory. According to Cartwright and Longuet-Higgins (1956), the peak of a random function can be calculated from its root mean square (rms) value by the approximate expression (valid for large  $N_z$ )

$$\frac{y_{\max}}{y_{\text{rms}}} = \sqrt{2 \ln N_z} + \left[ \frac{0.5772}{\sqrt{2 \ln N_z}} \right], \quad (26)$$

where  $N_z$  is the number of zero crossings in the time domain. A more accurate form of this equation used in SMSIM is given by

$$\frac{y_{\max}}{y_{\text{rms}}} = 2 \int_0^\infty (1 - [1 - \xi \exp(-z^2)] N_e) dz, \quad (27)$$

where  $\xi = N_z/N_e$  and  $N_e$  is the number of extrema in the time domain. From Parseval's theorem,  $y_{\text{rms}}$  is given by

$$y_{\text{rms}} = \left[ \frac{1}{T_{\text{rms}}} \int_0^\infty |Y(M_0, R, f)|^2 df \right]^{1/2}, \quad (28)$$

where  $T_{\text{rms}}$  is the equivalent rms duration. One of the critical elements of the above relation is the appropriate selection of  $T_{\text{rms}}$ . This is particularly critical at long periods and small magnitudes where the natural period can be longer than the duration of the time series. Methods for estimating  $T_{\text{rms}}$  that take into account the period of the oscillator are discussed by Boore and Joyner (1984), Liu and Pezeshk (1999), and Boore (2003). According to D. Boore (personal comm., 2001) SMSIM uses the method proposed by Boore and Joyner (1984) in which

$$T_{\text{rms}} = T_{\text{gm}} + T_0 \left( \frac{\gamma^3}{\gamma^3 + \frac{1}{3}} \right), \quad (29)$$

where  $\gamma = T_{\text{gm}}/T_0$ ; the ground-motion duration is given by  $T_{\text{gm}} = T_s + T_p$ , in which  $T_s$  is the duration of the source

and  $T_p$  is the duration of the path (Table 2), and the oscillator duration is given by  $T_0 = 1/(2\pi f_r \zeta)$ .

For this study representative stochastic model parameters for WNA (principally California), with the exception of  $\Delta\sigma$  and  $\kappa_0$ , were adopted from the point-source stochastic model of Atkinson and Silva (2000). This model uses the geometrical attenuation terms of Raoof *et al.* (1999) and the WNA generic-rock crustal velocity and amplification model of Boore and Joyner (1997). Although developed for southern California, the Raoof *et al.* crustal attenuation relation should be a reasonable estimate of WNA attenuation out to distances of 70 km for which the hybrid empirical estimates are made. For these distances any regional differences in anelastic attenuation in WNA should be negligible compared to the difference in anelastic attenuation between WNA and ENA. Atkinson and Silva selected  $\Delta\sigma = 80$  bar and  $\kappa_0 = 0.03$  sec to use in their model based on a comparison of the response spectra predicted from the Abrahamson and Silva (1997) ground-motion relation and the spectra predicted from a finite-fault stochastic simulation model for WNA. Boore and Joyner (1997) concluded that  $\Delta\sigma = 70$  bar and  $\kappa_0 = 0.035$  sec were reasonably consistent with the empirical spectra predicted from the Boore *et al.* (1997) ground-motion relation based on a comparison with their calculated stochastic response spectra for WNA. I selected  $\Delta\sigma = 100$  bar and  $\kappa_0 = 0.04$  sec because these values provided the best overall fit to all of the empirical attenuation relations (Boore and Joyner, 1997). Additional justification for these values is given in Figure 1.

Representative median values of the stochastic model parameters for ENA were taken from Atkinson and Boore (1998), with the exception of  $\beta_s$  and  $\Delta\sigma$ , which were taken from Frankel *et al.* (1996) in order to be consistent with my

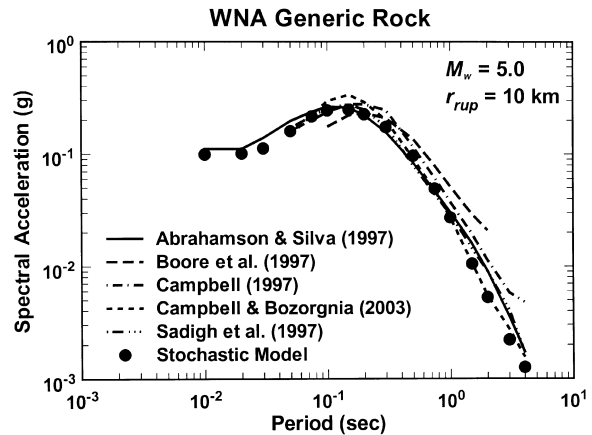


Figure 1. Comparison of 5% damped acceleration response spectra predicted from several widely used WNA empirical ground-motion relations with the spectrum predicted from a point-source  $\omega$ -square stochastic model with  $\Delta\sigma = 100$  bar,  $\kappa_0 = 0.04$  sec, and the WNA generic-rock site amplification model of Boore and Joyner (1997). The comparison is for  $M_w$  5.0 and a distance of 10 km.

use of a single-corner rather than a double-corner source spectrum. The use of  $\beta_s = 3.6$  km/sec and  $\Delta\sigma = 150$  bar with the one-corner source spectrum results in a high-frequency source spectral amplitude that is consistent with that used to develop the double-corner Atkinson and Boore ground-motion relation, which was constrained by seismological data. The ENA stochastic model uses the ENA hard-rock crustal velocity and amplification model of Boore and Joyner (1997), except that  $\kappa_0 = 0.006$  sec instead of 0.003 sec. The lower value was found by Atkinson (1996) for southeastern Canada. Nonetheless, I have retained the use of the higher value for now to be consistent with that proposed by EPRI (1993) for the Midcontinent region of ENA and adopted by the majority of the ENA ground-motion relations currently used in practice. The selected WNA and ENA stochastic model parameters are summarized in Tables 2–4.

I assumed that the epistemic uncertainty in the stochastic ground-motion estimates for WNA were negligible compared to those in ENA because the model parameters derived for this region are generally well constrained by both weak- and strong-motion recordings. This assumption is confirmed at least partially by comparing several WNA empirical response spectra for  $M_W = 5.0$  and  $r_{jb} = r_{rup} = r_{seis} = 10$  km with the stochastic WNA ground-motion estimates derived from the model parameters given in Tables 2–4. This comparison is shown in Figure 1. I am not suggesting that there is no epistemic uncertainty in WNA model parameters, but only that it is small compared to ENA and, therefore, can be neglected. All of the model parameters in ENA were estimated from weak-motion recordings from small magnitudes and large distances, which leads to significant epistemic uncertainty in the calculated strong ground motion. Following the approach used in the Trial Implementation Project (Savy *et al.*, 1999), I included epistemic uncertainty in the median values of  $\Delta\sigma$ ,  $Q(f)$ , and  $\kappa_0$  using alternative values recommended by EPRI (1993) and Toro *et al.* (1997). I considered the uncertainty in all of the other model parameters to be aleatory and, therefore, included as part of the WNA aleatory standard deviation. This brings up the ambiguity in trying to separate uncertainty into its aleatory and epistemic components. I have based my definition of aleatory variability on that used for the Yucca Mountain and Trial Implementation Projects. This definition could change in the future as research in this area progresses. Example values of the modeled ENA/WNA adjustment factors,  $F(\beta_{jk}, \phi_{lm}^t, \phi_{op}^h)$ , calculated from equation (4) for  $M_W = 6.5$  and  $R = 10$  km, showing their sensitivity to  $\Delta\sigma$  and  $\kappa_0$ , are given in Table 5.

I calculated the median hybrid empirical estimate of the ENA ground motion,  $\tilde{y}^{ena}(\beta_{jk})$ , from equation (1) for the set of magnitudes, distances, and ground-motion parameters used to derive the empirical estimates,  $y_i^{wna}(\beta_{jk})$ . I calculated the hybrid empirical estimate of the mean ENA aleatory standard deviation of ground motion,  $\bar{\sigma}_{ln y}^{ena}(\beta_{jk})$ , from equation (5), consistent with the methodology used in the Yucca Mountain and Trial Implementation Projects. I assumed that

Table 3  
Parameters of the Local Site Profiles Used in the WNA and ENA Stochastic Models

| Western North America (WNA) |                                |                           | Eastern North America (ENA) |                                |                           |
|-----------------------------|--------------------------------|---------------------------|-----------------------------|--------------------------------|---------------------------|
| Depth, $z$<br>(km)          | Velocity, $\beta$<br>(km/sec)* | Density, $\rho$<br>(g/cc) | Depth, $z$<br>(km)          | Velocity, $\beta$<br>(km/sec)* | Density, $\rho$<br>(g/cc) |
| $\leq 0.001$                | 0.245                          | 2.495                     | 0                           | 2.768                          | 2.731                     |
| 0.001–0.03                  | $2.206z^{0.272}$               | — <sup>†</sup>            | 0.05                        | 2.808                          | 2.735                     |
| 0.03–0.19                   | $3.542z^{0.407}$               | — <sup>†</sup>            | 0.10                        | 2.847                          | 2.739                     |
| 0.19–4.00                   | $2.505z^{0.199}$               | — <sup>†</sup>            | 0.15                        | 2.885                          | 2.742                     |
| 4.00–8.00                   | $2.927z^{0.086}$               | — <sup>†</sup>            | 0.20                        | 2.922                          | 2.746                     |
| $\geq 8.00$                 | 3.500                          | 2.800                     | 0.25                        | 2.958                          | 2.749                     |
|                             |                                |                           | 0.30                        | 2.993                          | 2.752                     |
|                             |                                |                           | 0.35                        | 3.026                          | 2.756                     |
|                             |                                |                           | 0.40                        | 3.059                          | 2.759                     |
|                             |                                |                           | 0.45                        | 3.091                          | 2.762                     |
|                             |                                |                           | 0.50                        | 3.122                          | 2.765                     |
|                             |                                |                           | 0.55                        | 3.151                          | 2.767                     |
|                             |                                |                           | 0.60                        | 3.180                          | 2.770                     |
|                             |                                |                           | 0.65                        | 3.208                          | 2.773                     |
|                             |                                |                           | 0.70                        | 3.234                          | 2.775                     |
|                             |                                |                           | 0.75                        | 3.260                          | 2.778                     |
|                             |                                |                           | 0.75–2.20                   | $3.324z^{0.067}$               | — <sup>†</sup>            |
|                             |                                |                           | 2.20–8.00                   | $3.447z^{0.0209}$              | — <sup>†</sup>            |
|                             |                                |                           | $\geq 8.00$                 | 3.6                            | 2.809                     |

\*Average shear-wave velocity in the upper 30 m is 620 m/sec for WNA and 2800 m/sec for ENA.

<sup>†</sup> $\rho = 2.5 + 0.09375(\beta - 0.3)$  g/cc.

Table 4  
Site Amplification Factors Estimated from the WNA and ENA Stochastic Models

| Western North America (WNA) |                            |                        | Eastern North America (ENA) |                            |                        |
|-----------------------------|----------------------------|------------------------|-----------------------------|----------------------------|------------------------|
| Frequency, $f$<br>(Hz)      | Amplification,<br>$A(f)^*$ | Site Term,<br>$G(f)^†$ | Frequency, $f$<br>(Hz)      | Amplification,<br>$A(f)^*$ | Site Term,<br>$G(f)^†$ |
| 0.01                        | 1.00                       | 1.00                   | 0.01                        | 1.00                       | 1.00                   |
| 0.09                        | 1.10                       | 1.09                   | 0.10                        | 1.02                       | 1.02                   |
| 0.16                        | 1.18                       | 1.16                   | 0.20                        | 1.03                       | 1.03                   |
| 0.51                        | 1.42                       | 1.33                   | 0.30                        | 1.05                       | 1.04                   |
| 0.84                        | 1.58                       | 1.42                   | 0.50                        | 1.07                       | 1.06                   |
| 1.25                        | 1.74                       | 1.49                   | 0.90                        | 1.09                       | 1.07                   |
| 2.26                        | 2.06                       | 1.55                   | 1.25                        | 1.11                       | 1.08                   |
| 3.17                        | 2.25                       | 1.51                   | 1.80                        | 1.12                       | 1.08                   |
| 6.05                        | 2.58                       | 1.21                   | 3.00                        | 1.13                       | 1.07                   |
| 16.60                       | 3.13                       | 0.39                   | 5.30                        | 1.14                       | 1.03                   |
| 61.20                       | 4.00                       | 0.00                   | 8.00                        | 1.15                       | 0.99                   |
|                             |                            |                        | 14.00                       | 1.15                       | 0.88                   |
|                             |                            |                        | 30.00                       | 1.15                       | 0.65                   |
|                             |                            |                        | 60.00                       | 1.15                       | 0.37                   |
|                             |                            |                        | 100.00                      | 1.15                       | 0.17                   |

\*Excludes the effects of  $\kappa_0$ . Amplification at other frequencies are obtained by interpolation assuming a linear dependence between log frequency and log amplification.

<sup>†</sup>Includes the effects of  $\kappa_0 = 0.04$  sec in WNA and  $\kappa_0 = 0.006$  sec in ENA.

Table 5  
Modeled ENA/WNA Adjustment Factors Showing  
the Effect of  $\kappa_0$  and  $\Delta\sigma$

| Period<br>(sec) | Adjustment Factor for $M_W$ 6.5, $R = 10$ km |                          |                          |                          |                          |
|-----------------|--|--------------------------|--------------------------|--------------------------|--------------------------|
|                 | $\kappa_0 = 0.003$ sec                       |                          | $\kappa_0 = 0.006$ sec   |                          | $\kappa_0 = 0.012$ sec   |
|                 | $\Delta\sigma = 150$ bar                     | $\Delta\sigma = 105$ bar | $\Delta\sigma = 150$ bar | $\Delta\sigma = 215$ bar | $\Delta\sigma = 150$ bar |
| 0.01            | 3.005  | 1.701                    | 2.261                    | 3.018                    | 1.568                    |
| 0.02            | 7.652  | 3.767                    | 5.040                    | 6.731                    | 2.470                    |
| 0.03            | 6.631  | 3.730                    | 4.964                    | 6.623                    | 2.895                    |
| 0.05            | 4.127  | 2.599                    | 3.453                    | 4.598                    | 2.444                    |
| 0.075           | 2.556  | 1.709                    | 2.266                    | 3.012                    | 1.789                    |
| 0.10            | 1.921  | 1.324                    | 1.754                    | 2.327                    | 1.466                    |
| 0.15            | 1.424  | 1.015                    | 1.340                    | 1.772                    | 1.187                    |
| 0.20            | 1.232  | 0.893                    | 1.176                    | 1.550                    | 1.073                    |
| 0.30            | 1.081  | 0.800                    | 1.048                    | 1.373                    | 0.986                    |
| 0.50            | 1.015  | 0.768                    | 0.997                    | 1.292                    | 0.960                    |
| 0.75            | 1.009  | 0.777                    | 0.997                    | 1.277                    | 0.973                    |
| 1.0             | 1.002  | 0.783                    | 0.994                    | 1.257                    | 0.976                    |
| 1.5             | 0.991  | 0.795                    | 0.987                    | 1.217                    | 0.977                    |
| 2.0             | 0.978  | 0.804                    | 0.977                    | 1.176                    | 0.972                    |
| 3.0             | 0.939  | 0.805                    | 0.941                    | 1.088                    | 0.942                    |
| 4.0             | 0.919  | 0.809                    | 0.921                    | 1.041                    | 0.924                    |

the distance measure used in the stochastic model,  $R$ , could be equated to the distance measure,  $r_{\text{rup}}$ , used in the development of the ENA ground-motion relations for purposes of deriving the modeled adjustment factors. This assumption is consistent with the recommendation of Boore (2003) for using stochastic modeling results to predict ground motions from large earthquakes.

One important limitation of the empirical ground-motion estimates, and therefore the hybrid empirical estimates, is their invalidity beyond distances of 60–100 km. Because of the lower rate of attenuation in ENA, ground motions of engineering significance can occur to distances of several hundred kilometers in this region. In order to overcome this limitation, the hybrid empirical estimates were supplemented with stochastic ENA estimates at  $R = 70, 100, 130, 200, 300, 500, 700$ , and 1000 km. This was done by scaling the stochastic estimates by the factor required to make the stochastic estimate at  $R = 70$  km equal to the median hybrid empirical estimate at  $r_{\text{rup}} = 70$  km for the same magnitude. These stochastic estimates were then used together with the hybrid empirical estimates in the regression analysis.

I used nonlinear least-squares regression to develop the ground-motion relations from the individual hybrid empirical ground-motion estimates. The functional form of this relation was developed by trial and error using functional forms proposed in previous studies until there was a sufficient match between the predicted and observed values. I used a similar approach to develop relations for the aleatory standard deviation. The resulting ground-motion relations are given by

$$\ln Y = c_1 + f_1(M_W) + f_2(M_W, r_{\text{rup}}) + f_3(r_{\text{rup}}), \quad (30)$$

where

$$f_1(M_W) = c_2 M_W + c_3 (8.5 - M_W)^2, \quad (31)$$

$$f_2(M_W, r_{\text{rup}}) = c_4 \ln R + (c_5 + c_6 M_W) r_{\text{rup}}, \quad (32)$$

$$R = \sqrt{r_{\text{rup}}^2 + [c_7 \exp(c_8 M_W)]^2}, \quad (33)$$

and

$$f_3(r_{\text{rup}}) = \begin{cases} 0 & \text{for } r_{\text{rup}} \leq r_1 \\ c_7(\ln r_{\text{rup}} - \ln r_1) & \text{for } r_1 < r_{\text{rup}} \leq r_2 \\ c_7(\ln r_{\text{rup}} - \ln r_1) + c_8(\ln r_{\text{rup}} - \ln r_2) & \text{for } r_{\text{rup}} > r_2 \end{cases} \quad (34)$$

In these equations  $Y$  is the geometric mean of the two horizontal components of PGA or 5% damped PSA in gravitational acceleration ( $g$ ),  $M_W$  is moment magnitude,  $r_{\text{rup}}$  is closest distance to fault rupture in kilometers,  $r_1 = 70$  km, and  $r_2 = 130$  km.

The relations for the aleatory standard deviation of ground motion are given by

$$\sigma_{\ln Y} = \begin{cases} c_{11} + c_{12} M_W & \text{for } M_W < M_1 \\ c_{13} & \text{for } M_W \geq M_1 \end{cases}, \quad (35)$$

where  $M_1 = 7.16$ .

The regression coefficients  $c_1$  through  $c_{13}$  are listed in Table 6. Figure 2 shows the magnitude and distance dependence of PGA and PSA at periods of 0.2, 1.0, and 3.0 sec predicted by equation (30), along with the individual hybrid empirical ground-motion estimates used in its development. Figure 3 shows a similar comparison of the 5% damped PSA response spectra. These figures indicate that the error involved in fitting equation (30) to the hybrid empirical estimates is very small and does not contribute measurably to the aleatory standard deviation. Equations for the epistemic standard deviations of  $\ln Y$  and  $\sigma_{\ln Y}$  were not developed in this study due to their complex functional forms. Instead they are tabulated in the Appendix for representative values of  $M_W$  and  $r_{\text{rup}}$ . I recommend, however, that epistemic uncertainty in predicted ground motion and aleatory standard deviation be taken into account by using the maximum of those derived from the use of multiple ENA ground-motion relations and those listed in the Appendix to ensure that this uncertainty is not underestimated. In regions where there are no multiple ground-motion relations, I would suggest using the standard deviations listed in the Appendix or calculating them by means of the mathematical framework presented previously.

Figure 4 compares the magnitude and distance scaling characteristics predicted by the ENA ground-motion relations developed in this study with the scaling characteristics predicted by the alternative hybrid empirical models developed by Atkinson (2001b) and Abrahamson and Silva (2001). Figure 5 gives a similar comparison for spectral acceleration. Since Atkinson (2001b) only developed a model

Table 6  
Regression Coefficients for the ENA Hybrid Empirical Ground-Motion Relation

| $T$ (sec) | $c_1$   | $c_2$ | $c_3$   | $c_4$  | $c_5$    | $c_6$    | $c_7$ | $c_8$ | $c_9$ | $c_{10}$ | $c_{11}$ | $c_{12}$ | $c_{13}$ |
|-----------|---------|-------|---------|--------|----------|----------|-------|-------|-------|----------|----------|----------|----------|
| 0.01      | 0.0305  | 0.633 | -0.0427 | -1.591 | -0.00428 | 0.000483 | 0.683 | 0.416 | 1.140 | -0.873   | 1.030    | -0.0860  | 0.414    |
| 0.02      | 1.3535  | 0.630 | -0.0404 | -1.787 | -0.00388 | 0.000497 | 1.020 | 0.363 | 0.851 | -0.715   | 1.030    | -0.0860  | 0.414    |
| 0.03      | 1.1860  | 0.622 | -0.0362 | -1.691 | -0.00367 | 0.000501 | 0.922 | 0.376 | 0.759 | -0.922   | 1.030    | -0.0860  | 0.414    |
| 0.05      | 0.3736  | 0.616 | -0.0353 | -1.469 | -0.00378 | 0.000500 | 0.630 | 0.423 | 0.771 | -1.239   | 1.042    | -0.0838  | 0.443    |
| 0.075     | -0.0395 | 0.615 | -0.0353 | -1.383 | -0.00421 | 0.000486 | 0.491 | 0.463 | 0.955 | -1.349   | 1.052    | -0.0838  | 0.453    |
| 0.10      | -0.1475 | 0.613 | -0.0353 | -1.369 | -0.00454 | 0.000460 | 0.484 | 0.467 | 1.096 | -1.284   | 1.059    | -0.0838  | 0.460    |
| 0.15      | -0.1901 | 0.616 | -0.0478 | -1.368 | -0.00473 | 0.000393 | 0.461 | 0.478 | 1.239 | -1.079   | 1.068    | -0.0838  | 0.469    |
| 0.20      | -0.4328 | 0.617 | -0.0586 | -1.320 | -0.00460 | 0.000337 | 0.399 | 0.493 | 1.250 | -0.928   | 1.077    | -0.0838  | 0.478    |
| 0.30      | -0.6906 | 0.609 | -0.0786 | -1.280 | -0.00414 | 0.000263 | 0.349 | 0.502 | 1.241 | -0.753   | 1.081    | -0.0838  | 0.482    |
| 0.50      | -0.5907 | 0.534 | -0.1379 | -1.216 | -0.00341 | 0.000194 | 0.318 | 0.503 | 1.166 | -0.606   | 1.098    | -0.0824  | 0.508    |
| 0.75      | -0.5429 | 0.480 | -0.1806 | -1.184 | -0.00288 | 0.000160 | 0.304 | 0.504 | 1.110 | -0.526   | 1.105    | -0.0806  | 0.528    |
| 1.0       | -0.6104 | 0.451 | -0.2090 | -1.158 | -0.00255 | 0.000141 | 0.299 | 0.503 | 1.067 | -0.482   | 1.110    | -0.0793  | 0.543    |
| 1.5       | -0.9666 | 0.441 | -0.2405 | -1.135 | -0.00213 | 0.000119 | 0.304 | 0.500 | 1.029 | -0.438   | 1.099    | -0.0771  | 0.547    |
| 2.0       | -1.4306 | 0.459 | -0.2552 | -1.124 | -0.00187 | 0.000103 | 0.310 | 0.499 | 1.015 | -0.417   | 1.093    | -0.0758  | 0.551    |
| 3.0       | -2.2331 | 0.492 | -0.2646 | -1.121 | -0.00154 | 0.000084 | 0.310 | 0.499 | 1.014 | -0.393   | 1.090    | -0.0737  | 0.562    |
| 4.0       | -2.7975 | 0.507 | -0.2738 | -1.119 | -0.00135 | 0.000074 | 0.294 | 0.506 | 1.018 | -0.386   | 1.092    | -0.0722  | 0.575    |

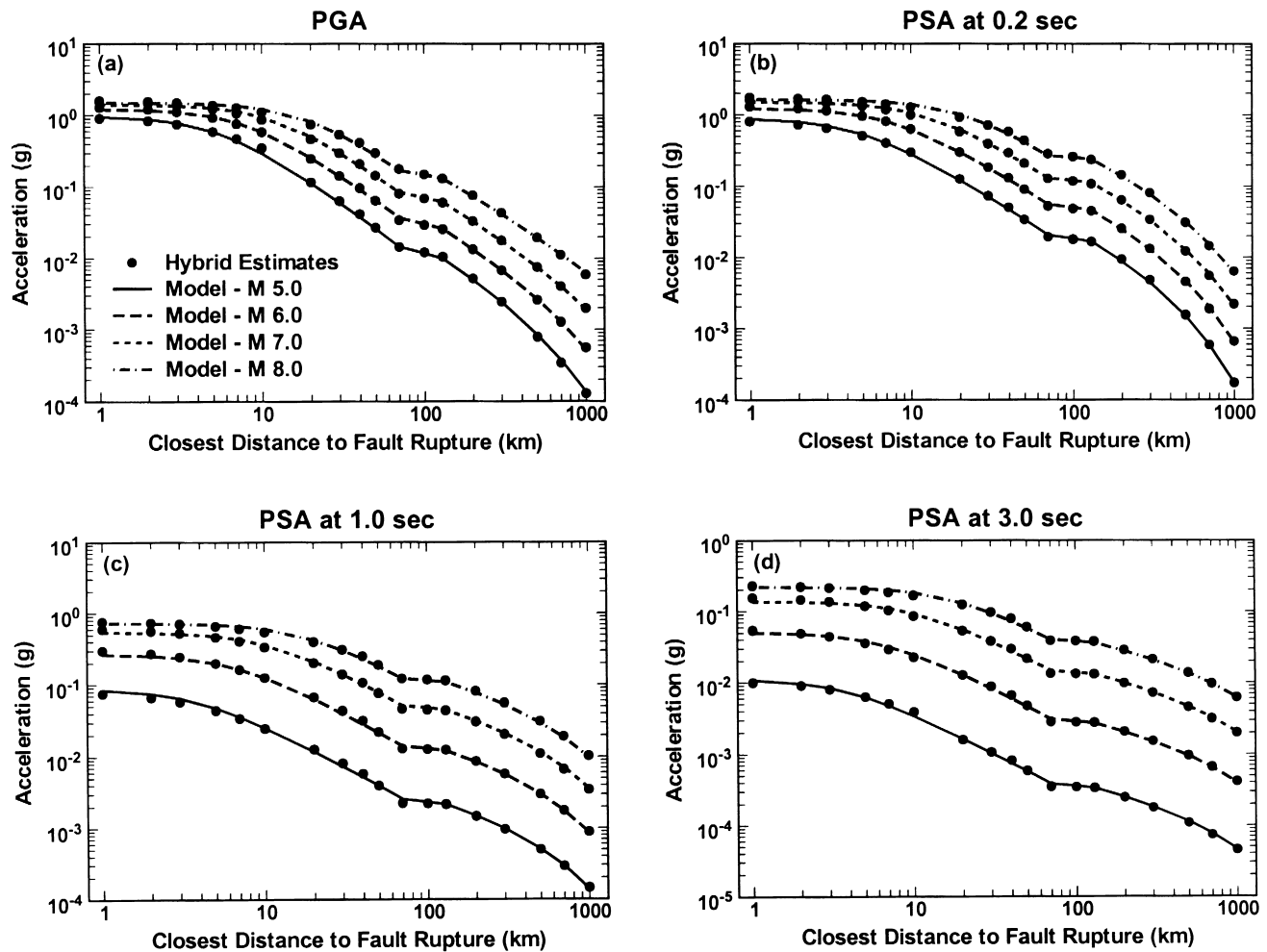


Figure 2. Plot of the hybrid empirical ground-motion relations for ENA hard rock developed in this study for (a) peak ground acceleration, (b) 5% damped response spectral acceleration at 0.2-sec period, (c) 5% damped response spectral acceleration at 1.0-sec period, and (d) 5% damped response spectral acceleration at 3.0-sec period. The individual hybrid empirical estimates are shown as solid circles.

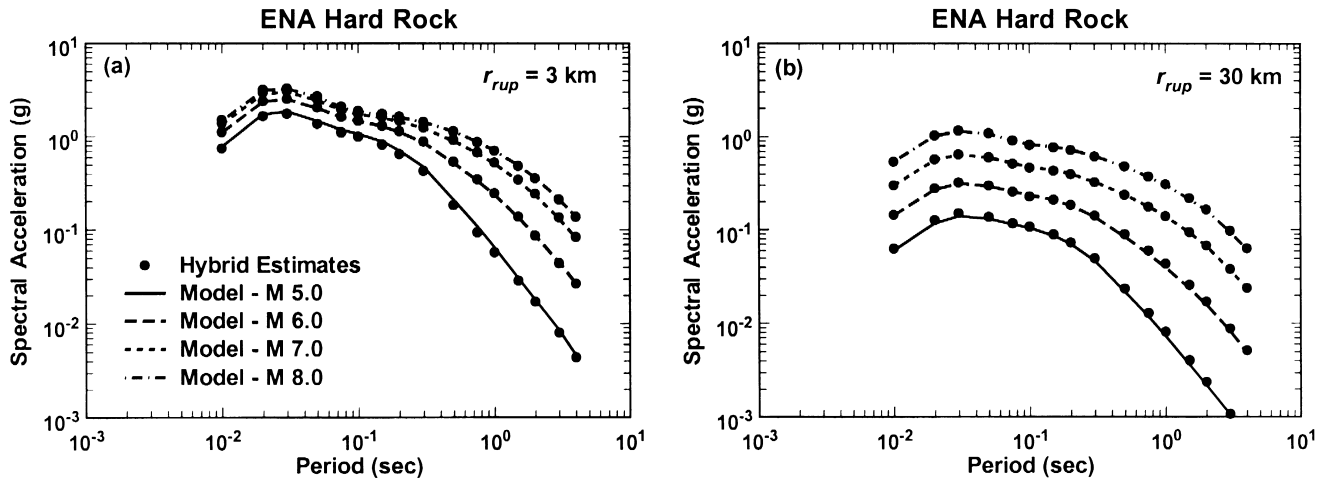


Figure 3. Plot of 5% damped acceleration response spectra for ENA hard rock predicted from the hybrid empirical ground-motion relations developed in this study for (a) a fault rupture distance of 3 km and (b) a fault rupture distance of 30 km. The individual hybrid empirical estimates are shown as solid circles.

for the ENA/WNA adjustment factors, I have applied her adjustment factors to the empirical ground-motion estimates developed in this study out to a distance of 70 km. Figures 6 and 7 give similar comparisons with the stochastic ENA ground-motion relations developed by Atkinson and Boore (1995, 1997), Frankel *et al.* (1996), Toro *et al.* (1997), and Savy *et al.* (1999) and with the theoretical ENA relation developed by Somerville *et al.* (2001). For simplicity all of these comparisons are made assuming a vertical fault. I used the equation rather than the tabulated version of the Atkinson and Boore relations, noting that they recommend the former when seismological parameters allow (e.g., for  $M_W \leq 7.25$  and hypocentral distances between 10 and 500 km). Since the Frankel *et al.* relations are given only in tabulated form, I truncated them at their minimum hypocentral distance of 10 km, noting that Frankel *et al.* (1996, 2002) used the ground-motion values at 10 km at shorter distances as well. The assumed hypocentral depth for the Atkinson and Boore and Frankel *et al.* relations is taken as 6 km for  $M_W$  5.5 and 12 km for  $M_W$  7.5 as recommended by Atkinson (2001b) based on the evaluation of Atkinson and Silva (2000). Assuming these hypocentral depths represent the center of the rupture plane (i.e., that the closest distance to the surface projection of the fault rupture plane,  $r_{jb}$ , can be substituted for epicentral distance as suggested by Boore [2003]), I calculated the remaining distance measures needed for the comparisons assuming that the depth to the top of the rupture plane is 3.2 km for  $M_W$  5.5 and at the ground surface for  $M_W$  7.5 based on the rupture width versus magnitude relation of Wells and Coppersmith (1994). The comparisons given in Figures 4–7 would be different, and possibly considerably different, if other assumptions regarding fault geometry and hypocentral and rupture depths were used, because of the inherent differences in the distance measures. A full evaluation of these differences is beyond the scope of this article.

The simplifying assumptions used in making the comparisons in Figures 4–7 prevent me from making general conclusions regarding the various ground-motion models. However, some differences are striking enough to warrant discussion. For example, the Abrahamson and Silva (2001) hybrid empirical model shows little anelastic attenuation at large distances. This latter model is based on the empirical WNA attenuation relation of Abrahamson and Silva (1997), which is not constrained by realistic anelastic attenuation rates at distances greater than about 100 km. Similar results were found in this study when the hybrid empirical estimates were not supplemented with stochastic simulations. The Atkinson (2001b) relation would actually begin to increase with distance if extended to larger distances, which is why she explicitly recommended that it not be used at distances greater than 100 km. The use of stochastic simulations to extend my relations beyond 70 km overcomes the problems exhibited by these other relations. These problems are not visible in the response spectral comparisons in Figure 5 because of the small distance that was used, but this figure does indicate that there is a considerable amount of variation among the different relations at short periods.

The comparisons in Figures 6 and 7 indicate that differences in ground motion predicted from the ENA stochastic and theoretical relations reach a factor of 5 or more. I believe that it is important to include this large degree of epistemic uncertainty in making ground-motion estimates in ENA. The ground-motion relations developed in this study predict the highest ground motion for  $M_W$  5.5 and  $r_{rup} < 10$  km, which I believe is due to the relatively shallow depth to fault rupture (3.2 km) used in the comparisons. This observation is consistent with the behavior of the empirical relations and, in my opinion, is appropriate for such a shallow source. Because of the high rate of attenuation predicted by the hybrid empirical model, a deeper source would likely reduce the

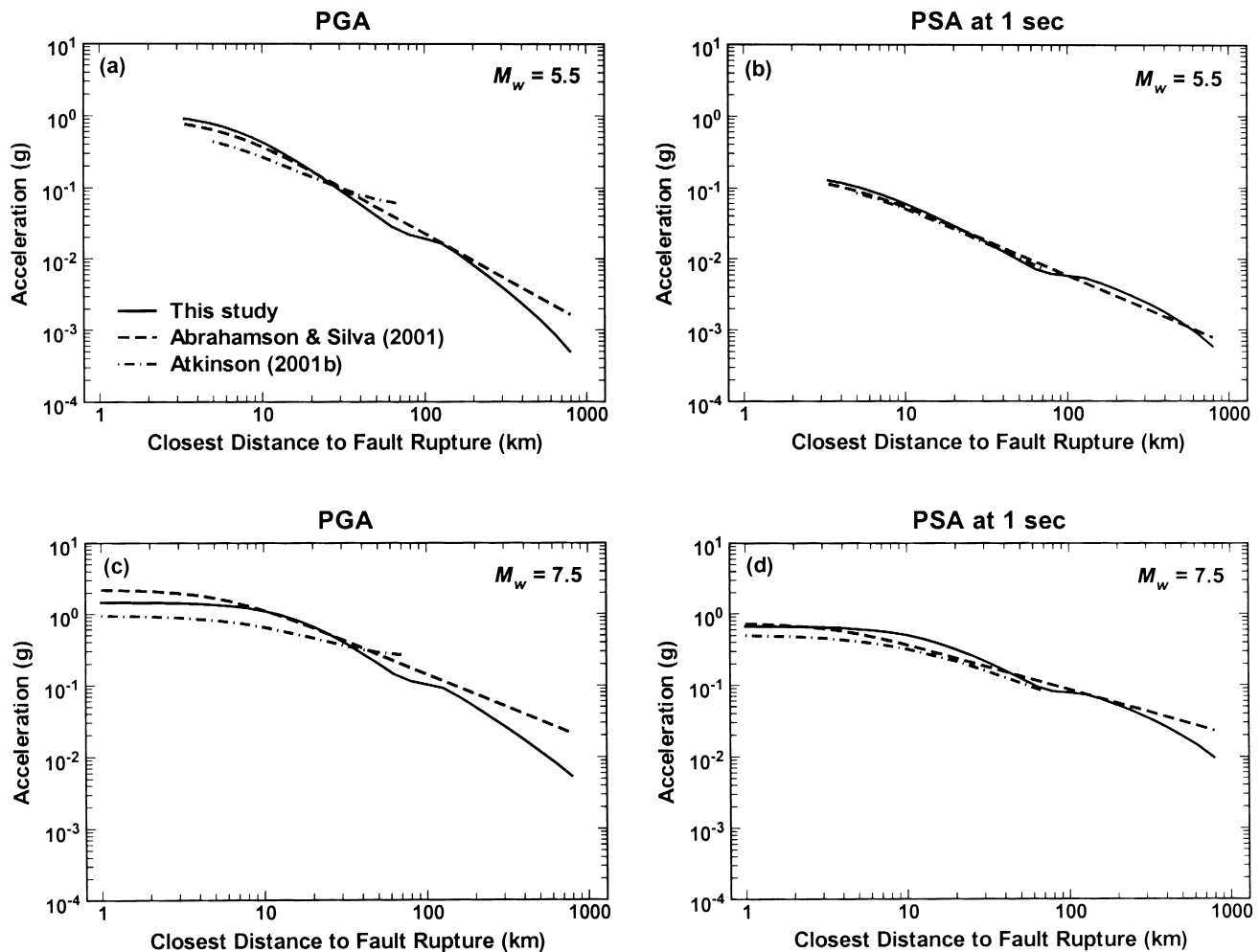


Figure 4. Comparison of several ENA hard-rock ground-motion relations that have been developed using the hybrid empirical method for (a) peak ground acceleration and  $M_w$  5.5, (b) 5% damped spectral acceleration at 1.0-sec period and  $M_w$  5.5, (c) peak ground acceleration and  $M_w$  7.5, (d) 5% damped spectral acceleration at 1.0-sec period and  $M_w$  7.5.

hybrid empirical estimates relative to the other models. The Somerville *et al.* (2001) attenuation relation predicts the lowest ground motion for  $M_w$  5.5; however, they did not recommend that their relation be used for  $M_w < 6$ . Since this relation, like that of Toro *et al.* (1997), uses the closest distance to the surface projection of fault rupture,  $r_{jb}$ , its predicted value is independent of source depth. So as source depth increases, ground motions from those relations that are based on fault or hypocentral distance will be reduced relative to the Somerville *et al.* and Toro *et al.* relations. Differences among the various ground-motion relations are smaller at  $M_w$  7.5, for which differences in the treatment of source depth are less important because of the relatively large rupture area. This strong dependence on source depth demonstrates the importance of using appropriate source depths when estimating ground motion from relations that use different distance measures. The Atkinson and Boore (1995, 1997) relations predict relatively low 1-sec val-

ues consistent with its use of a double-corner source spectrum. The double-corner spectrum appears to be supported by ENA recordings (Atkinson and Silva, 1997; Atkinson and Boore, 1998) but remains controversial. An advantage of the hybrid empirical method is that it possibly sidesteps this controversy by using the ratio of the modeled spectra between the host and target regions as opposed to the modeled spectra itself.

### Discussion

There are several factors that make the hybrid empirical method a viable alternative to the stochastic method traditionally used to estimate strong ground motion in areas such as ENA where there is a limited number of strong-motion recordings. The first factor is that it relies on empirical ground-motion relations that are generally well constrained by strong-motion recordings over the range of magnitudes

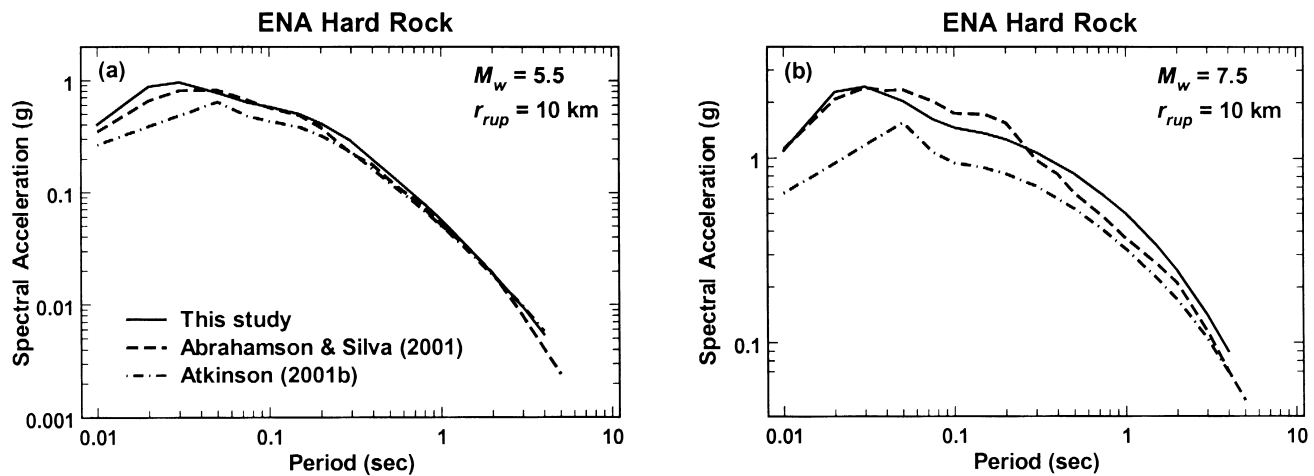


Figure 5. Comparison of 5% damped acceleration response spectra predicted from several ENA hard-rock ground-motion relations that have been developed using the hybrid empirical method for (a)  $M_w$  5.5 and (b)  $M_w$  7.5. The comparison is for a fault rupture distance of 10 km.

and distances of greatest engineering interest. As a result, the magnitude- and distance-scaling characteristics predicted by the method, at least in the near-source region, are strongly founded on observations rather than seismological models and assumptions. This aspect of the method is particularly important for ground-motion estimates close to large-magnitude earthquakes, which are strongly influenced by the complexities of fault geometry and rupture characteristics. More complex seismological models can be used to better predict these near-source effects, but it takes considerable computational effort to produce ground-motion estimates that account for the wide range in period, magnitude, distance, source geometry, stress drop, regional attenuation, crustal structure, local site characteristics, and other seismological parameters that are necessary to develop such regional ground-motion relations. These more complex models also require many more assumptions regarding model parameters than the simpler model used here, and many of these parameters must be questionably derived from earthquakes in WNA and other regions of abundant strong-motion recordings. As a result there have been only a few attempts to derive ground-motion relations using finite-fault rupture models (e.g., Atkinson and Silva, 2000; Somerville *et al.*, 2001; Gregor *et al.*, 2002) and only one of these was for ENA (Somerville *et al.*, 2001).

A second factor is that the hybrid empirical method uses relative differences in modeled ground motion between the host and target regions to derive the adjustment factors needed to apply empirical ground-motion relations in the target region. This helps to mitigate the additional uncertainty inherent in calculating absolute values of ground motion using stochastic and theoretical models alone. A third factor is that the method has the ability to provide explicitly, in a straightforward manner, estimates of aleatory variability (randomness) and epistemic uncertainty (lack of scientific

knowledge) in the predicted ground motions for the target region.

The application of the hybrid empirical method requires abundant and reliable seismological data for both the host and target regions. Therefore, it might not be possible to apply the method in some regions. A critical underlying assumption of the method is that the near-source scaling characteristics captured in the empirical ground-motion relations from the host region (e.g., WNA) are similar to those expected in the target region; that is, that such near-source characteristics can be considered regionally invariant. If this is not the case, then the method will not give reliable estimates of ground motion in the near-source region. One possible reason why empirically based near-source ground-motion characteristics would not be transferable to another region is that they include soil nonlinearity effects that are not taken into account in the calculation of the modeled adjustment factors. It is for this reason that I used empirical ground-motion relations for generic rock to derive the ENA ground-motion relations. However, WNA generic rock might also exhibit some nonlinearity at short periods because of its relatively low shear-wave velocity (e.g., Campbell, 2002, 2003).

There are several potential limitations in the hybrid empirical method as it has been applied in this study that bear mentioning. The first potential limitation is its use of a point-source single-corner  $\omega$ -square source spectrum (Brune, 1970, 1971) to derive the stochastic ground-motion estimates in WNA and ENA. However, this might only be an issue if one region has a different source-spectral shape than the other. For example, Atkinson and Silva (1997) proposed a double-corner source spectrum for California that they believe is more consistent with the strong-motion recordings in that region. Many other investigators (see the compilation in Atkinson and Boore [1998]) have also proposed double-

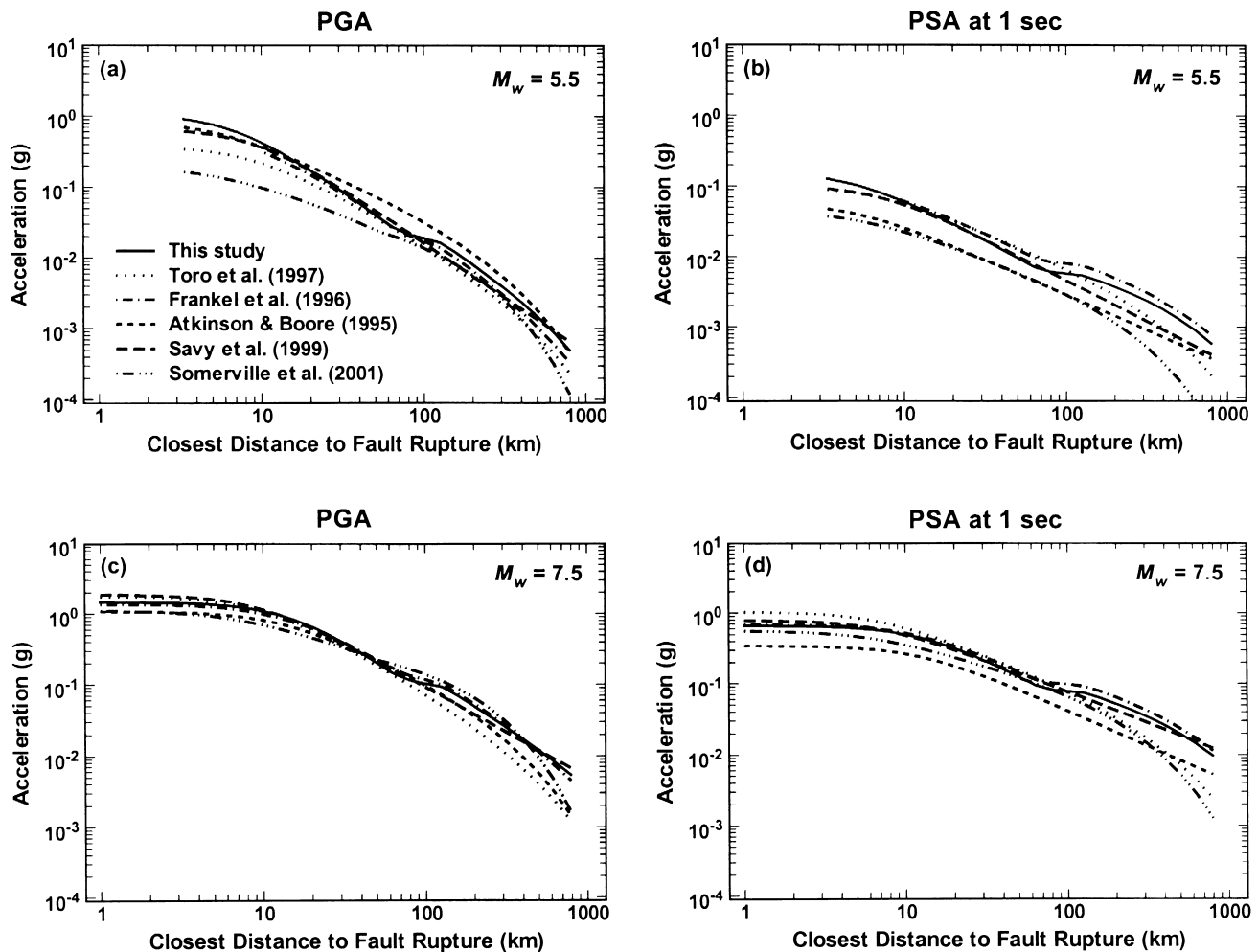


Figure 6. Comparison of several widely used ENA hard-rock ground-motion relations with the hybrid empirical ground-motion relations developed in this study for (a) peak ground acceleration and  $M_w$  5.5, (b) 5% damped response spectral acceleration at 1.0-sec period and  $M_w$  5.5, (c) peak ground acceleration and  $M_w$  7.5, (d) 5% damped response spectral acceleration at 1.0-sec period and  $M_w$  7.5.

corner source spectra for ENA. After using the finite-fault stochastic method to model several moderate to large earthquakes in ENA (Beresnev and Atkinson, 1999) and WNA (Beresnev and Atkinson, 2002), Beresnev and Atkinson (2002) suggested that a generic, region-independent earthquake source model could be developed for engineering prediction of strong ground motion. Based on these observations, I suggest that it might not matter whether a single-corner or a double-corner source spectrum, or for that matter whether a point-source or a finite-fault source model, is used to compute the stochastic ground motions used in the hybrid empirical method as long as the same type of model is valid in both the host and target regions. This hypothesis will be tested in a future study.

It is interesting to note that, although Atkinson and Silva (1997) found that their empirical source spectrum for California was similar to that for ENA at low frequencies when differences in crustal properties were taken into account,

they also found that the ENA source spectrum appears to have enhanced high-frequency amplitudes as compared to that in California. They suggest that these enhanced high-frequency amplitudes are consistent with known differences in stress drop between the two regions. I found generally similar characteristics in my modeled adjustment factors (see the adjustment factors for  $\Delta\sigma = 150$  bar and  $\kappa_0 = 0.006$  sec in Table 5). Therefore, differences in source spectra, aside from those caused by differences in stress drop, might not be very important in the development of modeled adjustment factors between WNA and ENA.

Atkinson (2001b) and Beresnev and Atkinson (2002) went one step further than Atkinson and Silva (1997) and suggested that there might be little, if any, difference in the apparent source radiation from ENA and WNA earthquakes of a given moment magnitude at high as well as low frequencies. For example, Atkinson cited a comparison of MMI data in these two regions by Hanks and Johnston (1992) that

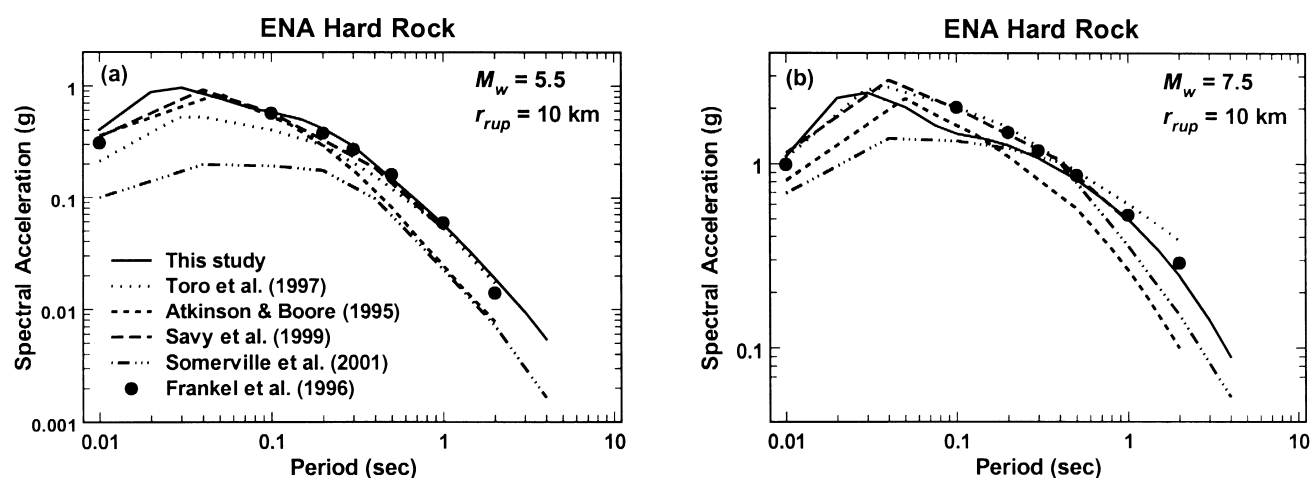


Figure 7. Comparison of 5% damped acceleration response spectra predicted from several widely used ENA hard-rock ground-motion relations with the spectra predicted from the hybrid empirical ground-motion relations developed in this study for (a)  $M_w$  5.5 and (b)  $M_w$  7.5. The comparison is for a distance of 10 km.

suggests that near-source damage levels, and by inference ground-motion levels, are similar in the two regions for the same moment magnitude. However, this inference is questionable considering that Hanks and Johnston conclude that the MMI data, especially at the intensity VII and higher level, are extremely limited and are not in themselves sufficient to rule out a factor of 2 higher stress drop in ENA. Bollinger *et al.* (1993) performed a similar study of MMI and concluded that the scatter in the MMI data was indeed large but that, in their opinion, it supported a factor of 2 higher stress drop in ENA. Atkinson and Boore (1998) used the stochastic method to modify the empirical California source model of Atkinson and Silva (1997) for differences in crustal properties and generic-rock site characteristics between California and ENA and found that this modified model matched the ENA strong-motion data almost as well as the Atkinson and Boore (1995, 1997) stochastic ENA ground-motion relations and better than many other ENA relations. Beresnev and Atkinson (2002) suggested that the observed difference in ground motion between the two regions can be explained entirely by regional differences in crustal properties and anelastic attenuation. However, there is a great deal of scatter in the inferred source spectra between WNA and ENA, which could easily obscure the 50% difference in stress drop that I have assumed between these two regions. Obviously there is still a great deal of controversy surrounding this issue, which should be taken into account with epistemic uncertainty.

A second potential limitation in the hybrid empirical method is that it can only provide reliable estimates of ground motion out to distances of 70–100 km because of the limitation in the empirical strong-motion database. Therefore, it must rely on modeled ground-motion estimates to extrapolate the hybrid empirical estimates beyond these distances where, for example, crustal reflections off the Moho and other significant crustal reflectors have been observed

to be important in both California (Somerville and Yoshimura, 1990; Campbell, 1991) and ENA (Burger *et al.*, 1987; Atkinson and Mereu, 1992; Atkinson and Boore, 1995, 1997). Fortunately, near-source effects are not as important at these distances, and the extrapolation of the hybrid empirical ground-motion estimates to larger distances using modeled ground motions in ENA, as proposed in this study, should be reasonably valid, particularly given the abundant seismological data used to constrain the attenuation rates at large distances in this region.

## Conclusions

In this study I have proposed a hybrid empirical method for estimating strong ground motion in regions of limited strong-motion recordings that is based on modifying empirical ground-motion (attenuation) relations from a host region (e.g., WNA) using modeled ground-motion ratios based on well-constrained seismological models between a host and target region (e.g., ENA). This method was used to develop ground-motion relations for ENA that compare favorably at moderate to large distances with other relations developed for the region. This comparison suggests that the hybrid empirical method is a viable alternative to the more traditional intensity, stochastic, and theoretical methods that are presently used to develop ground-motion relations in similar regions throughout the world. The method is especially useful for estimating strong ground motion near large-magnitude earthquakes. Although the method has been around for several decades, it has only recently gained credibility among seismologists as a viable alternative to the more traditional methods by evidence of its selection for the SSHAC (Budnitz *et al.*, 1997), Trial Implementation (Savy *et al.*, 1999), and Yucca Mountain (Stepp *et al.*, 2001) Projects and by its adaptation by Atkinson (2001b) and Abrahamson and Silva

(2001). I believe that the method, first proposed by Campbell (1981), is now mature enough to be used to develop alternative ground-motion relations in regions such as ENA where good seismological models and data are available.

By virtue of using modeled ground-motion ratios rather than absolute values, the hybrid empirical method is believed to sidestep some important controversial issues regarding ground-motion modeling in ENA and other stable continental regions, such as whether a single-corner or a double-corner source spectrum is appropriate and whether point-source or finite-fault rupture models are required. However, this requires further study. The method is particularly sensitive to the choice of the ratio of the stress drops ( $\Delta\sigma$ ) and near-surface attenuation factors ( $\kappa_0$ ) between the host and target regions, which themselves are the subject of considerable controversy. For the ground-motion relation developed in this study, the ratios of these parameters between ENA and WNA were assumed to be 1.5 (150 versus 100 bar) for  $\Delta\sigma$  and 0.15 (0.006 versus 0.04 sec) for  $\kappa_0$ . However, it should be noted that these ratios are controversial.

The ENA ground-motion relation developed in this study is considered to be valid for estimating ground motions for an ENA hard-rock site (a shear-wave velocity of 2800 m/sec) and for earthquakes of  $M_w$  5.0–8.2 and fault rupture distances of  $r_{\text{rup}} = 0$ –1000 km. If an estimate of ground motion for a different site condition is required, these estimates will need to be modified for the desired site condition using empirical or theoretical site factors. After review by an advisory panel, the USGS selected the ENA ground-motion relation developed in this study as one of five that it used in the 2002 update of the national seismic hazard maps (Frankel *et al.*, 2002). My comparison of several ground-motion relations in ENA indicated that the use of multiple relations, as was done by the USGS, is particularly important for this region since the differences in these predictions, a measure of epistemic uncertainty, can reach a factor of 5 or more, much larger than that found between empirical ground-motion relations in WNA.

## Acknowledgments

Gail Atkinson, Bob Youngs, and Dave Boore provided constructive comments. This research was supported by the U.S. Geological Survey (USGS), Department of the Interior, under USGS Award Number 01HQGR0011. The views and conclusions contained in this document are those of the author and should not be interpreted as necessarily representing the official policies, either expressed or implied, of the U.S. government.

## References

- Abrahamson, N. A., and K. M. Shedlock (1997). Overview, *Seism. Res. Lett.* **68**, 9–23.
- Abrahamson, N. A., and W. J. Silva (1997). Empirical response spectral attenuation relations for shallow crustal earthquakes, *Seism. Res. Lett.* **68**, 94–127.
- Abrahamson, N. A., and W. Silva (2001). “Empirical” attenuation relations for central and eastern U.S. hard and soft rock and deep soil site conditions, *Seism. Res. Lett.* **72**, 282.
- Anderson, J. G. (2003). Strong motion seismology, in *International Handbook of Earthquake and Engineering Seismology*, Part B, W. H. K. Lee, H. Kanamori, P. C. Jennings, and C. Kisslinger (Editors), Academic Press, London.
- Anderson, J. G., and S. E. Hough (1984). A model for the shape of the Fourier amplitude spectrum of acceleration at high frequencies, *Bull. Seism. Soc. Am.* **74**, 1969–1993.
- Atkinson, G. M. (1996). The high-frequency shape of the source spectrum for earthquakes in eastern and western Canada, *Bull. Seism. Soc. Am.* **86**, 106–112.
- Atkinson, G. M. (2001a). Linking historical intensity observations with ground-motion relations for eastern North America, *Seism. Res. Lett.* **72**, 560–574.
- Atkinson, G. M. (2001b). An alternative to stochastic ground-motion relations for use in seismic hazard analysis in eastern North America, *Seism. Res. Lett.* **72**, 299–306.
- Atkinson, G. M., and D. M. Boore (1995). New ground motion relations for eastern North America, *Bull. Seism. Soc. Am.* **85**, 17–30.
- Atkinson, G. M., and D. M. Boore (1997). Some comparisons between recent ground-motion relations, *Seism. Res. Lett.* **68**, 24–40.
- Atkinson, G. M., and D. M. Boore (1998). Evaluation of models for earthquake source spectra in eastern North America, *Bull. Seism. Soc. Am.* **88**, 917–934.
- Atkinson, G. M., and R. F. Mereu (1992). The shape of ground motion attenuation curves in southeastern Canada, *Bull. Seism. Soc. Am.* **82**, 2014–2031.
- Atkinson, G. M., and W. Silva (1997). An empirical study of earthquake source spectra for California earthquakes, *Bull. Seism. Soc. Am.* **87**, 97–113.
- Atkinson, G. M., and W. Silva (2000). Stochastic modeling of California ground motions, *Bull. Seism. Soc. Am.* **90**, 255–274.
- Atkinson, G. M., and E. Sonley (2000). Empirical relationships between Modified Mercalli Intensity and response spectra, *Bull. Seism. Soc. Am.* **90**, 537–544.
- Benjamin, J. R., and C. A. Cornell (1970). *Probability, Statistics, and Decision for Civil Engineers*, McGraw-Hill, New York.
- Beresnev, I. A., and G. M. Atkinson (1999). Generic finite-fault model for ground motion prediction in eastern North America, *Bull. Seism. Soc. Am.* **89**, 608–625.
- Beresnev, I. A., and G. M. Atkinson (2002). Source parameters of earthquakes in eastern and western North America based on finite-fault modeling, *Bull. Seism. Soc. Am.* **92**, 695–710.
- Bollinger, G. A., M. C. Chapman, and M. S. Sobol (1993). A comparison of earthquake damage areas as a function of magnitude across the United States, *Bull. Seism. Soc. Am.* **83**, 1064–1080.
- Bolt, B. A. (1987). *Seismic Strong Motion Synthetics*, Academic Press, New York.
- Boore, D. M. (1983). Stochastic simulation of high-frequency ground motion based on seismological models of the radiated spectra, *Bull. Seism. Soc. Am.* **73**, 1865–1893.
- Boore, D. M. (1996). SMSIM: Fortran programs for simulating ground motions from earthquakes, Version 1.0, *U.S. Geol. Surv. Open-File Rept.* 96-80-A.
- Boore, D. M. (2003). Prediction of ground motion using the stochastic method, *Pure Appl. Geophys.* **160**, 635–676.
- Boore, D. M., and W. B. Joyner (1984). A note on the use of random vibration theory to predict peak amplitudes of transient signals, *Bull. Seism. Soc. Am.* **74**, 2035–2039.
- Boore, D. M., and W. B. Joyner (1991). Estimation of ground motion at deep-soil sites in eastern North America, *Bull. Seism. Soc. Am.* **81**, 2167–2185.
- Boore, D. M., and W. B. Joyner (1997). Site amplification for generic rock sites, *Bull. Seism. Soc. Am.* **87**, 327–341.
- Boore, D. M., W. B. Joyner, and T. E. Fumal (1997). Equations for estimating horizontal response spectra and peak acceleration from western North American earthquakes: a summary of recent work, *Seism. Res. Lett.* **68**, 128–153.

- Brune, J. (1970). Tectonic stress and the spectra of seismic shear waves, *J. Geophys. Res.* **75**, 4997–5009.
- Brune, J. (1971). Correction: Tectonic stress and the spectra of seismic shear waves, *J. Geophys. Res.* **76**, 5002.
- Budnitz, R., G. Apostolakis, D. Boore, L. Cluff, K. Coppersmith, C. Cornell, and P. Morris (1997). Recommendations for probabilistic seismic hazard analysis: guidance on uncertainty and use of experts, NUREG/CR-6372, U.S. Nuclear Regulatory Commission, Washington, D.C.
- Burger, R. W., P. G. Somerville, J. S. Barker, R. B. Herrmann, and D. V. Helmberger (1987). The effect of crustal structure on strong ground motion attenuation relations in eastern North America, *Bull. Seism. Soc. Am.* **77**, 420–439.
- Campbell, K. W. (1981). A ground motion model for the central United States based on near-source acceleration data, in *Proc. of the Conference on Earthquakes and Earthquake Engineering: the Eastern United States*, Vol. 1, Ann Arbor Science Publishers, Ann Arbor, Michigan, 213–232.
- Campbell, K. W. (1982). A preliminary methodology for the regional zonation of peak ground acceleration, in *Proc. of the 3rd International Earthquake Microzonation Conference*, Univ. of Washington, Seattle, Vol. 1, 365–376.
- Campbell, K. W. (1986). An empirical estimate of near-source ground motion for a major,  $m_b = 6.8$ , earthquake in the eastern United States, *Bull. Seism. Soc. Am.* **76**, 1–17.
- Campbell, K. W. (1987). Predicting strong ground motion in Utah, in *Assessment of Regional Earthquake Hazards and Risk Along the Wasatch Front*, Utah, P. L. Gori and W. W. Hays (Editors), *U.S. Geol. Surv. Open-File Rept.* 87–585, Vol. 2, L1–L90.
- Campbell, K. W. (1991). An empirical analysis of peak horizontal acceleration for the Loma Prieta, California, earthquake of 18 October 1989, *Bull. Seism. Soc. Am.* **81**, 1838–1858.
- Campbell, K. W. (1997). Empirical near-source attenuation relationships for horizontal and vertical components of peak ground acceleration, peak ground velocity, and pseudo-absolute acceleration response spectra, *Seism. Res. Lett.* **68**, 154–179.
- Campbell, K. W. (2000a). Predicting strong ground motion in Utah, in *Assessment of Regional Earthquake Hazards and Risk Along the Wasatch Front*, Utah, P. L. Gori and W. W. Hays (Editors), *U.S. Geol. Surv. Profess. Paper* 1500-L, L1–L31.
- Campbell, K. W. (2000b). Erratum: Empirical near-source attenuation relationships for horizontal and vertical components of peak ground acceleration, peak ground velocity, and pseudo-absolute acceleration response spectra, *Seism. Res. Lett.* **71**, 353–355.
- Campbell, K. W. (2001a). Hybrid empirical model for estimating strong ground motion in regions of limited strong-motion recordings, in *Proc. of the OECD/NEA Workshop on the Engineering Characterization of Seismic Input*, Vol. 1, NEA/CSNI/R(2000)2, Nuclear Energy Agency, Paris, 315–332.
- Campbell, K. W. (2001b). Development of semi-empirical attenuation relationships for the CEUS, U.S. Geological Survey, Award 01HQGR0011, final report.
- Campbell, K. W. (2002). Engineering models of strong ground motion, in *Earthquake Engineering Handbook*, W. F. Chen and C. Scawthorn (Editors), CRC Press, Boca Raton, Florida, 5-1–5-76.
- Campbell, K. W. (2003). Strong motion attenuation relationships, in *International Handbook of Earthquake and Engineering Seismology*, Part B, W. H. K. Lee, H. Kanamori, P. C. Jennings, and C. Kisslinger (Editors), Academic Press, New York.
- Campbell, K. W., and Y. Bozorgnia (2003). Updated near-source ground-motion (attenuation) relations for the horizontal and vertical components of peak ground acceleration and acceleration response spectra, *Bull. Seism. Soc. Am.* **93**, 314–331.
- Cartwright, D. E., and M. S. Longuet-Higgins (1956). The statistical distribution of the maxima of a random function. *Proc. R. Soc. London A* **237**, 212–232.
- Electric Power Research Institute (EPRI) (1993). Methods and guidelines for estimating earthquake ground motion in eastern North America, in *Guidelines for Determining Design Basis Ground Motions*, Vol. 1, EPRI TR-102293, Electric Power Research Institute, Palo Alto, California.
- Frankel, A., C. Mueller, T. Barnhard, D. Perkins, E. Leyendecker, N. Dickman, S. Hanson, and M. Hopper (1996). National seismic hazard maps: documentation June 1996, *U.S. Geol. Surv. Open-File Rept.* 96-532.
- Frankel, A., M. Petersen, C. Mueller, K. Haller, R. Wheeler, E. Leyendecker, R. Wesson, S. Harmsen, C. Cramer, D. Perkins, and K. Ruks-ales (2002). Documentation of the 2002 update of the national seismic hazard maps, *U.S. Geol. Surv. Open-File Rept.* 02-420.
- Gregor, N. J., W. J. Silva, I. G. Wong, and R. R. Youngs (2002). Ground-motion attenuation relationships for Cascadia subduction zone megathrust earthquakes based on a stochastic finite-fault model, *Bull. Seism. Soc. Am.* **92**, 1923–1932.
- Hanks, T. C., and A. C. Johnston (1992). Common features of the excitation and propagation of strong ground motion for North American earthquakes, *Bull. Seism. Soc. Am.* **82**, 1–23.
- Hanks, T. C., and H. Kanamori (1979). A moment-magnitude scale, *J. Geophys. Res.* **84**, 2348–2350.
- Hanks, T. C., and R. K. McGuire (1981). The character of high-frequency strong ground motion, *Bull. Seism. Soc. Am.* **71**, 2071–2095.
- Joyner, W. B., R. E. Warrick, and T. E. Fumal (1981). The effect of Quaternary alluvium on strong ground motion in the Coyote Lake, California, earthquake of 1979, *Bull. Seism. Soc. Am.* **71**, 1333–1349.
- Liu, L., and S. Pezeshk (1999). An improvement on the estimation of pseudoresponse spectral velocity using RVT method, *Bull. Seism. Soc. Am.* **89**, 1384–1389.
- McGuire, R. K., and T. C. Hanks (1980). RMS accelerations and spectral amplitudes of strong ground motion during the San Fernando, California, earthquake, *Bull. Seism. Soc. Am.* **70**, 1907–1919.
- Newmark, N. M., and W. J. Hall (1982). *Earthquake Spectra and Design*, Earthquake Engineering Research Institute, Berkeley, California.
- Raoof, M., R. Herrmann, and L. Malagnini (1999). Attenuation and excitation of three-component ground motion in southern California, *Bull. Seism. Soc. Am.* **89**, 888–902.
- Sadigh, K., C. Y. Chang, J. A. Egan, F. Makdisi, and R. R. Youngs (1997). Attenuation relationships for shallow crustal earthquakes based on California strong motion data, *Seism. Res. Lett.* **68**, 180–189.
- Savy, J., W. Foxall, and N. Abrahamson (1999). Guidance for performing probabilistic seismic hazard analysis for a nuclear plant site: example application to the southeastern United States, NUREG/CR-6607, U.S. Nuclear Regulatory Commission, Washington, D.C.
- Silva, W., N. Gregor, and R. Darragh (2002). Development of regional hard rock attenuation relations for central and eastern North America, report prepared by Pacific Engineering and Analysis, El Cerrito, California.
- Somerville, P. (1993). Engineering applications of strong ground motion simulation, in *New Horizons in Strong Motion: Seismic Studies and Engineering Practice*, F. Lund (Editor), *Tectonophysics* **218**, 195–219.
- Somerville, P., and J. Yoshimura (1990). The influence of critical MOHO reflections on strong ground motions recorded in San Francisco and Oakland during the 1989 Loma Prieta earthquake, *Geophys. Res. Lett.* **17**, 1203–1206.
- Somerville, P., N. Collins, N. Abrahamson, R. Graves, and C. Saikia (2001). Ground motion attenuation relations for the central and eastern United States, U.S. Geological Survey, Award 99HQGR0098, final report.
- Stepp, J., I. Wong, J. Whitney, R. Quittmeyer, N. Abrahamson, G. Toro, R. Youngs, K. Coppersmith, J. Savy, T. Sullivan, and Yucca Mountain PSHA Project Members (2001). Probabilistic seismic hazard analyses for ground motions and fault displacement at Yucca Mountain, Nevada, *Earthquake Spectra* **17**, 113–151.
- Thenhaus, P. C., and K. W. Campbell (2002). Seismic hazard analysis, in

- Earthquake Engineering Handbook*, W. F. Chen and C. Scawthorn (Editors), CRC Press, Boca Raton, Florida, 8-1–8-50.
- Toro, G. R., N. A. Abrahamson, and J. F. Schneider (1997). Model of strong ground motions from earthquakes in central and eastern North America: best estimates and uncertainties, *Seism. Res. Lett.* **68**, 41–57.
- Trifunac, M. D., and V. W. Lee (1989). Empirical models for scaling pseudo relative velocity spectra of strong earthquake accelerations in terms of magnitude, distance, site intensity, and recording site conditions, *Soil Dyn. Earthquake Eng.* **8**, 126–144.
- Trifunac, M. D., and V. W. Lee (1992). A note on scaling peak acceleration, velocity, and displacement of strong earthquake shaking by Modified Mercalli Intensity (MMI) and site soil and geologic conditions, *Soil Dyn. Earthquake Eng.* **11**, 101–110.
- Wald, D. J., V. Quitoriano, T. H. Heaton, and H. Kanamori (1999). Relationships between peak ground acceleration, peak ground velocity, and Modified Mercalli Intensity in California, *Earthquake Spectra* **15**, 557–564.
- Wells, D. L., and K. J. Coppersmith (1994). New empirical relationships among magnitude, rupture length, rupture width, rupture area, and surface displacement, *Bull. Seism. Soc. Am.* **84**, 974–1002.

## Appendix

Table 1. Epistemic Standard Deviations of ENA Median Ground-Motion Values Derived Using the Hybrid Empirical Model

| $M_w$ | $r_{rup}$<br>(km) | Epistemic Standard Deviation (natural log) for Period (sec) |      |      |      |       |      |      |      |      |      |      |      |      |      |      |      |
|-------|-------------------|---|------|------|------|-------|------|------|------|------|------|------|------|------|------|------|------|
|       |                   | PGA   | 0.02 | 0.03 | 0.05 | 0.075 | 0.10 | 0.15 | 0.20 | 0.30 | 0.50 | 0.75 | 1.0  | 1.5  | 2.0  | 3.0  | 4.0  |
| 5.0   | 1                 | 0.39  | 0.53 | 0.39 | 0.28 | 0.22  | 0.20 | 0.20 | 0.23 | 0.30 | 0.27 | 0.26 | 0.24 | 0.31 | 0.33 | 0.37 | 0.60 |
| 5.0   | 2                 | 0.38  | 0.53 | 0.39 | 0.27 | 0.21  | 0.19 | 0.19 | 0.22 | 0.30 | 0.28 | 0.27 | 0.25 | 0.32 | 0.34 | 0.37 | 0.60 |
| 5.0   | 3                 | 0.38  | 0.52 | 0.39 | 0.27 | 0.21  | 0.18 | 0.18 | 0.21 | 0.29 | 0.27 | 0.26 | 0.25 | 0.31 | 0.34 | 0.37 | 0.59 |
| 5.0   | 5                 | 0.35  | 0.51 | 0.38 | 0.28 | 0.20  | 0.17 | 0.16 | 0.18 | 0.25 | 0.24 | 0.22 | 0.21 | 0.29 | 0.33 | 0.35 | 0.56 |
| 5.0   | 7                 | 0.34  | 0.49 | 0.37 | 0.28 | 0.20  | 0.17 | 0.15 | 0.16 | 0.22 | 0.20 | 0.18 | 0.18 | 0.26 | 0.30 | 0.32 | 0.52 |
| 5.0   | 10                | 0.32  | 0.48 | 0.36 | 0.28 | 0.21  | 0.18 | 0.16 | 0.15 | 0.19 | 0.15 | 0.13 | 0.13 | 0.23 | 0.28 | 0.28 | 0.46 |
| 5.0   | 20                | 0.29  | 0.47 | 0.36 | 0.28 | 0.24  | 0.23 | 0.21 | 0.18 | 0.16 | 0.11 | 0.07 | 0.06 | 0.16 | 0.23 | 0.20 | 0.33 |
| 5.0   | 30                | 0.30  | 0.47 | 0.37 | 0.30 | 0.27  | 0.27 | 0.24 | 0.23 | 0.17 | 0.15 | 0.11 | 0.10 | 0.16 | 0.22 | 0.16 | 0.27 |
| 5.0   | 40                | 0.32  | 0.48 | 0.39 | 0.33 | 0.30  | 0.30 | 0.27 | 0.26 | 0.20 | 0.20 | 0.16 | 0.14 | 0.17 | 0.22 | 0.14 | 0.23 |
| 5.0   | 50                | 0.34  | 0.49 | 0.42 | 0.36 | 0.34  | 0.34 | 0.29 | 0.30 | 0.24 | 0.25 | 0.20 | 0.17 | 0.18 | 0.22 | 0.13 | 0.21 |
| 5.0   | 70                | 0.39  | 0.52 | 0.47 | 0.42 | 0.40  | 0.39 | 0.34 | 0.36 | 0.30 | 0.32 | 0.27 | 0.23 | 0.21 | 0.24 | 0.13 | 0.21 |
| 5.4   | 1                 | 0.35  | 0.50 | 0.38 | 0.28 | 0.24  | 0.22 | 0.21 | 0.20 | 0.22 | 0.22 | 0.22 | 0.22 | 0.27 | 0.29 | 0.33 | 0.50 |
| 5.4   | 2                 | 0.35  | 0.51 | 0.38 | 0.28 | 0.23  | 0.21 | 0.20 | 0.20 | 0.22 | 0.23 | 0.23 | 0.23 | 0.29 | 0.31 | 0.34 | 0.50 |
| 5.4   | 3                 | 0.35  | 0.50 | 0.38 | 0.28 | 0.23  | 0.20 | 0.18 | 0.19 | 0.22 | 0.23 | 0.24 | 0.23 | 0.29 | 0.31 | 0.34 | 0.50 |
| 5.4   | 5                 | 0.34  | 0.50 | 0.38 | 0.29 | 0.22  | 0.18 | 0.16 | 0.17 | 0.20 | 0.21 | 0.22 | 0.22 | 0.28 | 0.31 | 0.33 | 0.49 |
| 5.4   | 7                 | 0.33  | 0.49 | 0.37 | 0.29 | 0.22  | 0.18 | 0.15 | 0.15 | 0.18 | 0.19 | 0.19 | 0.19 | 0.26 | 0.30 | 0.31 | 0.46 |
| 5.4   | 10                | 0.31  | 0.48 | 0.37 | 0.29 | 0.22  | 0.18 | 0.15 | 0.13 | 0.15 | 0.15 | 0.15 | 0.16 | 0.23 | 0.27 | 0.28 | 0.41 |
| 5.4   | 20                | 0.28  | 0.46 | 0.36 | 0.29 | 0.24  | 0.21 | 0.18 | 0.16 | 0.12 | 0.11 | 0.09 | 0.10 | 0.18 | 0.23 | 0.21 | 0.30 |
| 5.4   | 30                | 0.28  | 0.45 | 0.37 | 0.31 | 0.26  | 0.24 | 0.21 | 0.20 | 0.15 | 0.13 | 0.11 | 0.11 | 0.17 | 0.22 | 0.17 | 0.23 |
| 5.4   | 40                | 0.29  | 0.46 | 0.38 | 0.33 | 0.29  | 0.28 | 0.24 | 0.23 | 0.18 | 0.18 | 0.15 | 0.14 | 0.18 | 0.22 | 0.16 | 0.20 |
| 5.4   | 50                | 0.31  | 0.46 | 0.40 | 0.36 | 0.32  | 0.31 | 0.27 | 0.27 | 0.21 | 0.22 | 0.19 | 0.18 | 0.19 | 0.23 | 0.15 | 0.18 |
| 5.4   | 70                | 0.35  | 0.48 | 0.45 | 0.42 | 0.38  | 0.37 | 0.33 | 0.33 | 0.28 | 0.29 | 0.26 | 0.23 | 0.23 | 0.26 | 0.16 | 0.17 |
| 5.8   | 1                 | 0.33  | 0.49 | 0.38 | 0.30 | 0.28  | 0.27 | 0.25 | 0.23 | 0.17 | 0.17 | 0.18 | 0.19 | 0.22 | 0.23 | 0.26 | 0.37 |
| 5.8   | 2                 | 0.33  | 0.49 | 0.38 | 0.30 | 0.27  | 0.25 | 0.24 | 0.22 | 0.18 | 0.19 | 0.20 | 0.20 | 0.24 | 0.25 | 0.28 | 0.39 |
| 5.8   | 3                 | 0.33  | 0.49 | 0.38 | 0.30 | 0.26  | 0.24 | 0.22 | 0.21 | 0.18 | 0.19 | 0.20 | 0.21 | 0.25 | 0.26 | 0.28 | 0.39 |
| 5.8   | 5                 | 0.33  | 0.49 | 0.38 | 0.30 | 0.25  | 0.22 | 0.20 | 0.19 | 0.17 | 0.19 | 0.20 | 0.20 | 0.25 | 0.27 | 0.29 | 0.39 |
| 5.8   | 7                 | 0.32  | 0.49 | 0.38 | 0.31 | 0.24  | 0.21 | 0.18 | 0.17 | 0.16 | 0.18 | 0.18 | 0.19 | 0.24 | 0.27 | 0.28 | 0.38 |
| 5.8   | 10                | 0.31  | 0.48 | 0.38 | 0.31 | 0.24  | 0.20 | 0.16 | 0.15 | 0.14 | 0.16 | 0.16 | 0.17 | 0.23 | 0.25 | 0.26 | 0.35 |
| 5.8   | 20                | 0.28  | 0.46 | 0.37 | 0.31 | 0.25  | 0.21 | 0.18 | 0.16 | 0.14 | 0.13 | 0.13 | 0.14 | 0.19 | 0.22 | 0.20 | 0.25 |
| 5.8   | 30                | 0.27  | 0.45 | 0.37 | 0.32 | 0.27  | 0.24 | 0.21 | 0.20 | 0.16 | 0.15 | 0.14 | 0.15 | 0.19 | 0.22 | 0.18 | 0.20 |
| 5.8   | 40                | 0.28  | 0.45 | 0.38 | 0.34 | 0.30  | 0.27 | 0.25 | 0.24 | 0.20 | 0.19 | 0.18 | 0.18 | 0.21 | 0.24 | 0.18 | 0.18 |
| 5.8   | 50                | 0.30  | 0.45 | 0.40 | 0.37 | 0.33  | 0.30 | 0.28 | 0.27 | 0.24 | 0.23 | 0.21 | 0.21 | 0.23 | 0.25 | 0.19 | 0.17 |
| 5.8   | 70                | 0.34  | 0.47 | 0.45 | 0.43 | 0.39  | 0.37 | 0.34 | 0.34 | 0.30 | 0.30 | 0.28 | 0.27 | 0.27 | 0.29 | 0.21 | 0.18 |
| 6.2   | 1                 | 0.32  | 0.49 | 0.38 | 0.31 | 0.31  | 0.30 | 0.30 | 0.27 | 0.18 | 0.14 | 0.14 | 0.15 | 0.17 | 0.17 | 0.20 | 0.27 |
| 6.2   | 2                 | 0.32  | 0.49 | 0.38 | 0.31 | 0.29  | 0.29 | 0.28 | 0.26 | 0.17 | 0.15 | 0.15 | 0.15 | 0.18 | 0.18 | 0.21 | 0.28 |
| 6.2   | 3                 | 0.32  | 0.49 | 0.38 | 0.30 | 0.28  | 0.27 | 0.26 | 0.24 | 0.17 | 0.15 | 0.15 | 0.16 | 0.18 | 0.19 | 0.22 | 0.29 |
| 6.2   | 5                 | 0.32  | 0.49 | 0.38 | 0.30 | 0.26  | 0.24 | 0.23 | 0.21 | 0.16 | 0.16 | 0.16 | 0.16 | 0.19 | 0.20 | 0.23 | 0.29 |
| 6.2   | 7                 | 0.32  | 0.48 | 0.38 | 0.30 | 0.25  | 0.22 | 0.20 | 0.19 | 0.15 | 0.15 | 0.16 | 0.17 | 0.20 | 0.21 | 0.23 | 0.29 |
| 6.2   | 10                | 0.31  | 0.48 | 0.38 | 0.30 | 0.24  | 0.21 | 0.18 | 0.17 | 0.15 | 0.15 | 0.15 | 0.16 | 0.19 | 0.21 | 0.22 | 0.28 |
| 6.2   | 20                | 0.28  | 0.46 | 0.37 | 0.30 | 0.25  | 0.21 | 0.18 | 0.17 | 0.16 | 0.14 | 0.13 | 0.14 | 0.16 | 0.18 | 0.17 | 0.21 |
| 6.2   | 30                | 0.27  | 0.45 | 0.37 | 0.31 | 0.26  | 0.23 | 0.21 | 0.20 | 0.18 | 0.16 | 0.15 | 0.15 | 0.17 | 0.19 | 0.15 | 0.16 |
| 6.2   | 40                | 0.27  | 0.45 | 0.38 | 0.33 | 0.29  | 0.26 | 0.24 | 0.24 | 0.22 | 0.19 | 0.18 | 0.18 | 0.19 | 0.21 | 0.16 | 0.14 |
| 6.2   | 50                | 0.29  | 0.45 | 0.40 | 0.36 | 0.32  | 0.29 | 0.27 | 0.28 | 0.25 | 0.23 | 0.21 | 0.21 | 0.21 | 0.23 | 0.17 | 0.14 |
| 6.2   | 70                | 0.32  | 0.46 | 0.44 | 0.42 | 0.38  | 0.35 | 0.33 | 0.34 | 0.32 | 0.30 | 0.28 | 0.27 | 0.27 | 0.28 | 0.21 | 0.16 |
| 6.6   | 1                 | 0.32  | 0.49 | 0.38 | 0.32 | 0.34  | 0.33 | 0.33 | 0.31 | 0.22 | 0.15 | 0.13 | 0.12 | 0.14 | 0.14 | 0.17 | 0.20 |
| 6.6   | 2                 | 0.32  | 0.49 | 0.38 | 0.31 | 0.32  | 0.31 | 0.31 | 0.29 | 0.20 | 0.14 | 0.13 | 0.13 | 0.14 | 0.15 | 0.18 | 0.21 |

(continued)

Appendix, Table 1 (Continued)

| $M_W$ | $r_{rup}$<br>(km) | Epistemic Standard Deviation (natural log) for Period (sec) |      |      |      |       |      |      |      |      |      |      |      |      |      |      |      |
|-------|-------------------|---|------|------|------|-------|------|------|------|------|------|------|------|------|------|------|------|
|       |                   | PGA   | 0.02 | 0.03 | 0.05 | 0.075 | 0.10 | 0.15 | 0.20 | 0.30 | 0.50 | 0.75 | 1.0  | 1.5  | 2.0  | 3.0  | 4.0  |
| 6.6   | 3                 | 0.32  | 0.48 | 0.38 | 0.30 | 0.30  | 0.29 | 0.29 | 0.27 | 0.19 | 0.14 | 0.13 | 0.13 | 0.15 | 0.15 | 0.18 | 0.21 |
| 6.6   | 5                 | 0.31  | 0.48 | 0.37 | 0.30 | 0.27  | 0.26 | 0.25 | 0.24 | 0.17 | 0.14 | 0.13 | 0.13 | 0.15 | 0.15 | 0.18 | 0.21 |
| 6.6   | 7                 | 0.31  | 0.48 | 0.37 | 0.29 | 0.26  | 0.24 | 0.22 | 0.21 | 0.16 | 0.14 | 0.14 | 0.14 | 0.16 | 0.16 | 0.18 | 0.22 |
| 6.6   | 10                | 0.30  | 0.47 | 0.37 | 0.29 | 0.24  | 0.22 | 0.19 | 0.18 | 0.16 | 0.15 | 0.14 | 0.14 | 0.16 | 0.16 | 0.18 | 0.21 |
| 6.6   | 20                | 0.28  | 0.46 | 0.36 | 0.29 | 0.24  | 0.21 | 0.18 | 0.18 | 0.17 | 0.15 | 0.14 | 0.13 | 0.14 | 0.14 | 0.14 | 0.17 |
| 6.6   | 30                | 0.26  | 0.44 | 0.36 | 0.29 | 0.25  | 0.22 | 0.20 | 0.20 | 0.19 | 0.16 | 0.15 | 0.15 | 0.14 | 0.15 | 0.13 | 0.13 |
| 6.6   | 40                | 0.26  | 0.44 | 0.37 | 0.31 | 0.27  | 0.24 | 0.23 | 0.23 | 0.23 | 0.19 | 0.18 | 0.18 | 0.17 | 0.18 | 0.14 | 0.12 |
| 6.6   | 50                | 0.27  | 0.44 | 0.38 | 0.33 | 0.29  | 0.27 | 0.26 | 0.27 | 0.26 | 0.23 | 0.21 | 0.21 | 0.20 | 0.21 | 0.16 | 0.13 |
| 6.6   | 70                | 0.31  | 0.44 | 0.42 | 0.39 | 0.35  | 0.33 | 0.32 | 0.34 | 0.33 | 0.30 | 0.28 | 0.27 | 0.26 | 0.27 | 0.21 | 0.17 |
| 7.0   | 1                 | 0.32  | 0.49 | 0.38 | 0.31 | 0.33  | 0.33 | 0.34 | 0.33 | 0.23 | 0.16 | 0.13 | 0.13 | 0.14 | 0.15 | 0.17 | 0.17 |
| 7.0   | 2                 | 0.32  | 0.48 | 0.38 | 0.30 | 0.31  | 0.31 | 0.32 | 0.31 | 0.22 | 0.15 | 0.13 | 0.13 | 0.14 | 0.15 | 0.17 | 0.18 |
| 7.0   | 3                 | 0.31  | 0.48 | 0.37 | 0.29 | 0.30  | 0.29 | 0.30 | 0.29 | 0.20 | 0.15 | 0.13 | 0.13 | 0.15 | 0.16 | 0.18 | 0.18 |
| 7.0   | 5                 | 0.30  | 0.48 | 0.37 | 0.28 | 0.27  | 0.26 | 0.26 | 0.25 | 0.18 | 0.14 | 0.13 | 0.13 | 0.15 | 0.16 | 0.18 | 0.19 |
| 7.0   | 7                 | 0.30  | 0.47 | 0.36 | 0.27 | 0.25  | 0.23 | 0.22 | 0.21 | 0.16 | 0.14 | 0.13 | 0.14 | 0.16 | 0.16 | 0.18 | 0.19 |
| 7.0   | 10                | 0.29  | 0.47 | 0.36 | 0.27 | 0.23  | 0.21 | 0.19 | 0.18 | 0.16 | 0.15 | 0.14 | 0.14 | 0.15 | 0.15 | 0.17 | 0.19 |
| 7.0   | 20                | 0.27  | 0.45 | 0.36 | 0.26 | 0.22  | 0.20 | 0.17 | 0.17 | 0.17 | 0.16 | 0.14 | 0.14 | 0.13 | 0.13 | 0.14 | 0.15 |
| 7.0   | 30                | 0.26  | 0.44 | 0.35 | 0.27 | 0.22  | 0.20 | 0.18 | 0.19 | 0.19 | 0.17 | 0.15 | 0.15 | 0.13 | 0.13 | 0.12 | 0.13 |
| 7.0   | 40                | 0.25  | 0.43 | 0.36 | 0.28 | 0.24  | 0.21 | 0.21 | 0.22 | 0.22 | 0.20 | 0.18 | 0.17 | 0.15 | 0.16 | 0.14 | 0.13 |
| 7.0   | 50                | 0.25  | 0.42 | 0.37 | 0.30 | 0.26  | 0.24 | 0.23 | 0.25 | 0.25 | 0.23 | 0.21 | 0.20 | 0.19 | 0.20 | 0.16 | 0.15 |
| 7.0   | 70                | 0.28  | 0.43 | 0.39 | 0.35 | 0.31  | 0.29 | 0.29 | 0.32 | 0.32 | 0.29 | 0.28 | 0.27 | 0.25 | 0.26 | 0.22 | 0.19 |
| 7.4   | 1                 | 0.32  | 0.49 | 0.38 | 0.31 | 0.33  | 0.33 | 0.35 | 0.34 | 0.26 | 0.18 | 0.15 | 0.14 | 0.13 | 0.14 | 0.15 | 0.15 |
| 7.4   | 2                 | 0.32  | 0.49 | 0.38 | 0.30 | 0.31  | 0.31 | 0.33 | 0.33 | 0.24 | 0.17 | 0.14 | 0.13 | 0.13 | 0.14 | 0.15 | 0.15 |
| 7.4   | 3                 | 0.31  | 0.48 | 0.37 | 0.29 | 0.30  | 0.29 | 0.31 | 0.30 | 0.22 | 0.16 | 0.14 | 0.13 | 0.14 | 0.15 | 0.16 | 0.16 |
| 7.4   | 5                 | 0.30  | 0.47 | 0.37 | 0.28 | 0.27  | 0.26 | 0.27 | 0.26 | 0.19 | 0.15 | 0.14 | 0.14 | 0.16 | 0.17 | 0.18 | 0.18 |
| 7.4   | 7                 | 0.29  | 0.47 | 0.36 | 0.27 | 0.24  | 0.23 | 0.23 | 0.22 | 0.17 | 0.15 | 0.14 | 0.15 | 0.17 | 0.17 | 0.19 | 0.19 |
| 7.4   | 10                | 0.28  | 0.46 | 0.36 | 0.26 | 0.23  | 0.21 | 0.20 | 0.19 | 0.16 | 0.15 | 0.15 | 0.16 | 0.17 | 0.17 | 0.19 | 0.20 |
| 7.4   | 20                | 0.27  | 0.45 | 0.35 | 0.25 | 0.21  | 0.19 | 0.17 | 0.16 | 0.17 | 0.17 | 0.16 | 0.16 | 0.15 | 0.15 | 0.16 | 0.17 |
| 7.4   | 30                | 0.26  | 0.44 | 0.35 | 0.26 | 0.21  | 0.19 | 0.17 | 0.18 | 0.19 | 0.18 | 0.17 | 0.16 | 0.15 | 0.14 | 0.15 | 0.16 |
| 7.4   | 40                | 0.25  | 0.43 | 0.35 | 0.26 | 0.22  | 0.20 | 0.19 | 0.20 | 0.22 | 0.20 | 0.19 | 0.18 | 0.16 | 0.17 | 0.16 | 0.17 |
| 7.4   | 50                | 0.25  | 0.42 | 0.36 | 0.28 | 0.24  | 0.22 | 0.21 | 0.23 | 0.25 | 0.23 | 0.22 | 0.21 | 0.19 | 0.20 | 0.18 | 0.18 |
| 7.4   | 70                | 0.26  | 0.41 | 0.38 | 0.33 | 0.28  | 0.26 | 0.27 | 0.30 | 0.32 | 0.30 | 0.28 | 0.27 | 0.26 | 0.27 | 0.23 | 0.23 |
| 7.8   | 1                 | 0.32  | 0.49 | 0.39 | 0.31 | 0.34  | 0.33 | 0.36 | 0.36 | 0.28 | 0.21 | 0.17 | 0.15 | 0.13 | 0.14 | 0.14 | 0.15 |
| 7.8   | 2                 | 0.32  | 0.49 | 0.38 | 0.30 | 0.32  | 0.32 | 0.34 | 0.34 | 0.26 | 0.19 | 0.16 | 0.15 | 0.13 | 0.14 | 0.14 | 0.15 |
| 7.8   | 3                 | 0.31  | 0.48 | 0.38 | 0.29 | 0.30  | 0.30 | 0.33 | 0.32 | 0.25 | 0.18 | 0.16 | 0.14 | 0.14 | 0.15 | 0.15 | 0.16 |
| 7.8   | 5                 | 0.30  | 0.48 | 0.37 | 0.28 | 0.27  | 0.26 | 0.28 | 0.28 | 0.22 | 0.17 | 0.15 | 0.15 | 0.15 | 0.16 | 0.17 | 0.18 |
| 7.8   | 7                 | 0.29  | 0.47 | 0.36 | 0.26 | 0.25  | 0.24 | 0.25 | 0.24 | 0.19 | 0.16 | 0.15 | 0.15 | 0.17 | 0.18 | 0.19 | 0.20 |
| 7.8   | 10                | 0.28  | 0.46 | 0.35 | 0.25 | 0.22  | 0.21 | 0.21 | 0.20 | 0.18 | 0.17 | 0.17 | 0.17 | 0.18 | 0.19 | 0.20 | 0.21 |
| 7.8   | 20                | 0.27  | 0.45 | 0.35 | 0.25 | 0.21  | 0.19 | 0.17 | 0.17 | 0.18 | 0.18 | 0.18 | 0.18 | 0.18 | 0.18 | 0.19 | 0.21 |
| 7.8   | 30                | 0.26  | 0.44 | 0.35 | 0.25 | 0.21  | 0.19 | 0.17 | 0.18 | 0.20 | 0.20 | 0.19 | 0.18 | 0.18 | 0.18 | 0.18 | 0.20 |
| 7.8   | 40                | 0.25  | 0.43 | 0.35 | 0.26 | 0.21  | 0.19 | 0.18 | 0.20 | 0.22 | 0.21 | 0.20 | 0.20 | 0.19 | 0.19 | 0.19 | 0.20 |
| 7.8   | 50                | 0.24  | 0.42 | 0.35 | 0.27 | 0.22  | 0.20 | 0.20 | 0.22 | 0.25 | 0.24 | 0.23 | 0.22 | 0.21 | 0.22 | 0.20 | 0.22 |
| 7.8   | 70                | 0.25  | 0.41 | 0.37 | 0.31 | 0.26  | 0.24 | 0.25 | 0.29 | 0.31 | 0.30 | 0.29 | 0.28 | 0.27 | 0.28 | 0.25 | 0.26 |
| 8.2   | 1                 | 0.33  | 0.50 | 0.39 | 0.32 | 0.34  | 0.34 | 0.37 | 0.38 | 0.30 | 0.23 | 0.19 | 0.17 | 0.15 | 0.15 | 0.15 | 0.17 |
| 8.2   | 2                 | 0.33  | 0.49 | 0.39 | 0.31 | 0.33  | 0.33 | 0.36 | 0.36 | 0.28 | 0.22 | 0.18 | 0.17 | 0.15 | 0.15 | 0.15 | 0.17 |
| 8.2   | 3                 | 0.32  | 0.49 | 0.38 | 0.30 | 0.31  | 0.31 | 0.34 | 0.34 | 0.27 | 0.20 | 0.18 | 0.16 | 0.15 | 0.15 | 0.16 | 0.18 |
| 8.2   | 5                 | 0.30  | 0.48 | 0.37 | 0.28 | 0.28  | 0.27 | 0.30 | 0.30 | 0.24 | 0.19 | 0.17 | 0.16 | 0.16 | 0.17 | 0.17 | 0.19 |
| 8.2   | 7                 | 0.29  | 0.47 | 0.36 | 0.27 | 0.25  | 0.24 | 0.26 | 0.26 | 0.21 | 0.18 | 0.17 | 0.17 | 0.17 | 0.18 | 0.19 | 0.21 |
| 8.2   | 10                | 0.28  | 0.46 | 0.36 | 0.26 | 0.23  | 0.22 | 0.22 | 0.22 | 0.19 | 0.18 | 0.18 | 0.18 | 0.19 | 0.20 | 0.21 | 0.23 |
| 8.2   | 20                | 0.27  | 0.45 | 0.36 | 0.25 | 0.21  | 0.19 | 0.17 | 0.17 | 0.19 | 0.20 | 0.20 | 0.20 | 0.21 | 0.21 | 0.22 | 0.24 |
| 8.2   | 30                | 0.26  | 0.44 | 0.36 | 0.25 | 0.21  | 0.19 | 0.17 | 0.18 | 0.20 | 0.21 | 0.21 | 0.21 | 0.21 | 0.21 | 0.21 | 0.23 |
| 8.2   | 40                | 0.25  | 0.43 | 0.35 | 0.26 | 0.21  | 0.19 | 0.18 | 0.20 | 0.22 | 0.23 | 0.22 | 0.22 | 0.21 | 0.21 | 0.21 | 0.23 |
| 8.2   | 50                | 0.25  | 0.42 | 0.36 | 0.27 | 0.22  | 0.20 | 0.19 | 0.22 | 0.25 | 0.25 | 0.24 | 0.23 | 0.23 | 0.23 | 0.23 | 0.24 |
| 8.2   | 70                | 0.25  | 0.41 | 0.37 | 0.30 | 0.25  | 0.23 | 0.24 | 0.28 | 0.31 | 0.31 | 0.30 | 0.29 | 0.28 | 0.29 | 0.27 | 0.28 |

Table 2. Epistemic Standard Deviations of ENA Mean Aleatory Standard Deviation Values Derived Using the Hybrid Empirical Model

(continued)

Appendix, Table 2 (Continued)

| $M_W$ | $r_{rup}$<br>(km) | Epistemic Standard Deviation (natural log) for Period (sec) |      |      |      |       |      |      |      |      |      |      |      |      |      |      |      |
|-------|-------------------|---|------|------|------|-------|------|------|------|------|------|------|------|------|------|------|------|
|       |                   | PGA   | 0.02 | 0.03 | 0.05 | 0.075 | 0.10 | 0.15 | 0.20 | 0.30 | 0.50 | 0.75 | 1.0  | 1.5  | 2.0  | 3.0  | 4.0  |
| 7.0   | 7                 | 0.02  | 0.02 | 0.02 | 0.03 | 0.03  | 0.03 | 0.03 | 0.03 | 0.02 | 0.02 | 0.03 | 0.04 | 0.04 | 0.05 | 0.06 | 0.07 |
| 7.0   | 10                | 0.02  | 0.02 | 0.02 | 0.03 | 0.03  | 0.03 | 0.03 | 0.03 | 0.02 | 0.02 | 0.03 | 0.04 | 0.04 | 0.05 | 0.06 | 0.07 |
| 7.0   | 20                | 0.02  | 0.02 | 0.02 | 0.03 | 0.03  | 0.03 | 0.03 | 0.03 | 0.02 | 0.02 | 0.03 | 0.04 | 0.04 | 0.05 | 0.06 | 0.07 |
| 7.0   | 30                | 0.02  | 0.02 | 0.02 | 0.03 | 0.03  | 0.03 | 0.03 | 0.03 | 0.02 | 0.02 | 0.03 | 0.04 | 0.04 | 0.05 | 0.06 | 0.07 |
| 7.0   | 40                | 0.02  | 0.02 | 0.02 | 0.03 | 0.03  | 0.03 | 0.03 | 0.03 | 0.02 | 0.02 | 0.03 | 0.04 | 0.04 | 0.05 | 0.06 | 0.07 |
| 7.0   | 50                | 0.02  | 0.02 | 0.02 | 0.03 | 0.03  | 0.03 | 0.03 | 0.03 | 0.02 | 0.02 | 0.03 | 0.04 | 0.04 | 0.05 | 0.06 | 0.07 |
| 7.0   | 70                | 0.02  | 0.02 | 0.02 | 0.03 | 0.03  | 0.03 | 0.03 | 0.03 | 0.02 | 0.02 | 0.03 | 0.04 | 0.04 | 0.05 | 0.06 | 0.07 |
| 7.4   | 1                 | 0.04  | 0.04 | 0.04 | 0.04 | 0.04  | 0.04 | 0.04 | 0.04 | 0.03 | 0.03 | 0.04 | 0.05 | 0.05 | 0.06 | 0.07 | 0.08 |
| 7.4   | 2                 | 0.04  | 0.04 | 0.04 | 0.04 | 0.04  | 0.04 | 0.04 | 0.04 | 0.03 | 0.03 | 0.04 | 0.05 | 0.05 | 0.06 | 0.07 | 0.08 |
| 7.4   | 3                 | 0.04  | 0.04 | 0.04 | 0.04 | 0.04  | 0.04 | 0.04 | 0.04 | 0.03 | 0.03 | 0.04 | 0.05 | 0.05 | 0.06 | 0.07 | 0.08 |
| 7.4   | 5                 | 0.04  | 0.04 | 0.04 | 0.04 | 0.04  | 0.04 | 0.04 | 0.04 | 0.03 | 0.03 | 0.04 | 0.05 | 0.05 | 0.06 | 0.07 | 0.08 |
| 7.4   | 7                 | 0.04  | 0.04 | 0.04 | 0.04 | 0.04  | 0.04 | 0.04 | 0.04 | 0.03 | 0.03 | 0.04 | 0.05 | 0.05 | 0.06 | 0.07 | 0.08 |
| 7.4   | 10                | 0.04  | 0.04 | 0.04 | 0.04 | 0.04  | 0.04 | 0.04 | 0.04 | 0.03 | 0.03 | 0.04 | 0.05 | 0.05 | 0.06 | 0.07 | 0.08 |
| 7.4   | 20                | 0.04  | 0.04 | 0.04 | 0.04 | 0.04  | 0.04 | 0.04 | 0.04 | 0.03 | 0.03 | 0.04 | 0.05 | 0.05 | 0.06 | 0.07 | 0.08 |
| 7.4   | 30                | 0.04  | 0.04 | 0.04 | 0.04 | 0.04  | 0.04 | 0.04 | 0.04 | 0.03 | 0.03 | 0.04 | 0.05 | 0.05 | 0.06 | 0.07 | 0.08 |
| 7.4   | 40                | 0.04  | 0.04 | 0.04 | 0.04 | 0.04  | 0.04 | 0.04 | 0.04 | 0.03 | 0.03 | 0.04 | 0.05 | 0.05 | 0.06 | 0.07 | 0.08 |
| 7.4   | 50                | 0.04  | 0.04 | 0.04 | 0.04 | 0.04  | 0.04 | 0.04 | 0.04 | 0.03 | 0.03 | 0.04 | 0.05 | 0.05 | 0.06 | 0.07 | 0.08 |
| 7.4   | 70                | 0.04  | 0.04 | 0.04 | 0.04 | 0.04  | 0.04 | 0.04 | 0.04 | 0.03 | 0.03 | 0.04 | 0.05 | 0.05 | 0.06 | 0.07 | 0.08 |
| 7.8   | 1                 | 0.04  | 0.04 | 0.04 | 0.04 | 0.04  | 0.04 | 0.04 | 0.04 | 0.03 | 0.03 | 0.04 | 0.05 | 0.05 | 0.06 | 0.07 | 0.08 |
| 7.8   | 2                 | 0.04  | 0.04 | 0.04 | 0.04 | 0.04  | 0.04 | 0.04 | 0.04 | 0.03 | 0.03 | 0.04 | 0.05 | 0.05 | 0.06 | 0.07 | 0.08 |
| 7.8   | 3                 | 0.04  | 0.04 | 0.04 | 0.04 | 0.04  | 0.04 | 0.04 | 0.04 | 0.03 | 0.03 | 0.04 | 0.05 | 0.05 | 0.06 | 0.07 | 0.08 |
| 7.8   | 5                 | 0.04  | 0.04 | 0.04 | 0.04 | 0.04  | 0.04 | 0.04 | 0.04 | 0.03 | 0.03 | 0.04 | 0.05 | 0.05 | 0.06 | 0.07 | 0.08 |
| 7.8   | 7                 | 0.04  | 0.04 | 0.04 | 0.04 | 0.04  | 0.04 | 0.04 | 0.04 | 0.03 | 0.03 | 0.04 | 0.05 | 0.05 | 0.06 | 0.07 | 0.08 |
| 7.8   | 10                | 0.04  | 0.04 | 0.04 | 0.04 | 0.04  | 0.04 | 0.04 | 0.04 | 0.03 | 0.03 | 0.04 | 0.05 | 0.05 | 0.06 | 0.07 | 0.08 |
| 7.8   | 20                | 0.04  | 0.04 | 0.04 | 0.04 | 0.04  | 0.04 | 0.04 | 0.04 | 0.03 | 0.03 | 0.04 | 0.05 | 0.05 | 0.06 | 0.07 | 0.08 |
| 7.8   | 30                | 0.04  | 0.04 | 0.04 | 0.04 | 0.04  | 0.04 | 0.04 | 0.04 | 0.03 | 0.03 | 0.04 | 0.05 | 0.05 | 0.06 | 0.07 | 0.08 |
| 7.8   | 40                | 0.04  | 0.04 | 0.04 | 0.04 | 0.04  | 0.04 | 0.04 | 0.04 | 0.03 | 0.03 | 0.04 | 0.05 | 0.05 | 0.06 | 0.07 | 0.08 |
| 7.8   | 50                | 0.04  | 0.04 | 0.04 | 0.04 | 0.04  | 0.04 | 0.04 | 0.04 | 0.03 | 0.03 | 0.04 | 0.05 | 0.05 | 0.06 | 0.07 | 0.08 |
| 7.8   | 70                | 0.04  | 0.04 | 0.04 | 0.04 | 0.04  | 0.04 | 0.04 | 0.04 | 0.03 | 0.03 | 0.04 | 0.05 | 0.05 | 0.06 | 0.07 | 0.08 |
| 8.2   | 1                 | 0.04  | 0.04 | 0.04 | 0.04 | 0.04  | 0.04 | 0.04 | 0.04 | 0.03 | 0.03 | 0.04 | 0.05 | 0.05 | 0.06 | 0.07 | 0.08 |
| 8.2   | 2                 | 0.04  | 0.04 | 0.04 | 0.04 | 0.04  | 0.04 | 0.04 | 0.04 | 0.03 | 0.03 | 0.04 | 0.05 | 0.05 | 0.06 | 0.07 | 0.08 |
| 8.2   | 3                 | 0.04  | 0.04 | 0.04 | 0.04 | 0.04  | 0.04 | 0.04 | 0.04 | 0.03 | 0.03 | 0.04 | 0.05 | 0.05 | 0.06 | 0.07 | 0.08 |
| 8.2   | 5                 | 0.04  | 0.04 | 0.04 | 0.04 | 0.04  | 0.04 | 0.04 | 0.04 | 0.03 | 0.03 | 0.04 | 0.05 | 0.05 | 0.06 | 0.07 | 0.08 |
| 8.2   | 7                 | 0.04  | 0.04 | 0.04 | 0.04 | 0.04  | 0.04 | 0.04 | 0.04 | 0.03 | 0.03 | 0.04 | 0.05 | 0.05 | 0.06 | 0.07 | 0.08 |
| 8.2   | 10                | 0.04  | 0.04 | 0.04 | 0.04 | 0.04  | 0.04 | 0.04 | 0.04 | 0.03 | 0.03 | 0.04 | 0.05 | 0.05 | 0.06 | 0.07 | 0.08 |
| 8.2   | 20                | 0.04  | 0.04 | 0.04 | 0.04 | 0.04  | 0.04 | 0.04 | 0.04 | 0.03 | 0.03 | 0.04 | 0.05 | 0.05 | 0.06 | 0.07 | 0.08 |
| 8.2   | 30                | 0.04  | 0.04 | 0.04 | 0.04 | 0.04  | 0.04 | 0.04 | 0.04 | 0.03 | 0.03 | 0.04 | 0.05 | 0.05 | 0.06 | 0.07 | 0.08 |
| 8.2   | 40                | 0.04  | 0.04 | 0.04 | 0.04 | 0.04  | 0.04 | 0.04 | 0.04 | 0.03 | 0.03 | 0.04 | 0.05 | 0.05 | 0.06 | 0.07 | 0.08 |
| 8.2   | 50                | 0.04  | 0.04 | 0.04 | 0.04 | 0.04  | 0.04 | 0.04 | 0.04 | 0.03 | 0.03 | 0.04 | 0.05 | 0.05 | 0.06 | 0.07 | 0.08 |
| 8.2   | 70                | 0.04  | 0.04 | 0.04 | 0.04 | 0.04  | 0.04 | 0.04 | 0.04 | 0.03 | 0.03 | 0.04 | 0.05 | 0.05 | 0.06 | 0.07 | 0.08 |

ABS Consulting Inc. and EQECAT Inc.  
 1030 NW 161st Place  
 Beaverton, Oregon 97006  
[kcampbell@abconsulting.com](mailto:kcampbell@abconsulting.com)

Manuscript received 10 January 2002.